

NATO Lecture Series SCI-175

Frequency-Domain Design/Analysis of Robust Flight Control Systems

Ronald A. Hess

Dept. of Mechanical and Aeronautical Engineering

University of California

Davis, CA

USA

Acknowledgement

The research summarized herein would not have been possible without the contributions of the following students:

- Lt. Col. Scott Wells (Ph.D. 2002)
- Mr. Travis Vetter (MS 2002)
- Mr. Troy Ussery (MS 2003)
- Ms. Christina Spaulding (MS 2005)
- Ms. Maryam Bakhtiari-Nejad (MS 2006)
- Mr. Gianluca Cama (Diploma Eng. 2007)

Outline

- Introduction
- Overview of Sliding Mode Control (SMC)
- Frequency-Domain SMC Interpretation
- Overview of Human Pilot Modeling
- Flight Control Design Examples
- Summary

Problems, Challenges (and Warnings) in Flight Control System Design

“I believe the day is near at hand when the flyer will be almost entirely relieved of the work of maintaining the equilibrium of his machine”

-Orville Wright, 1914, *The Papers of Wilbur and Orville Wright*, McGraw-Hill, 1953

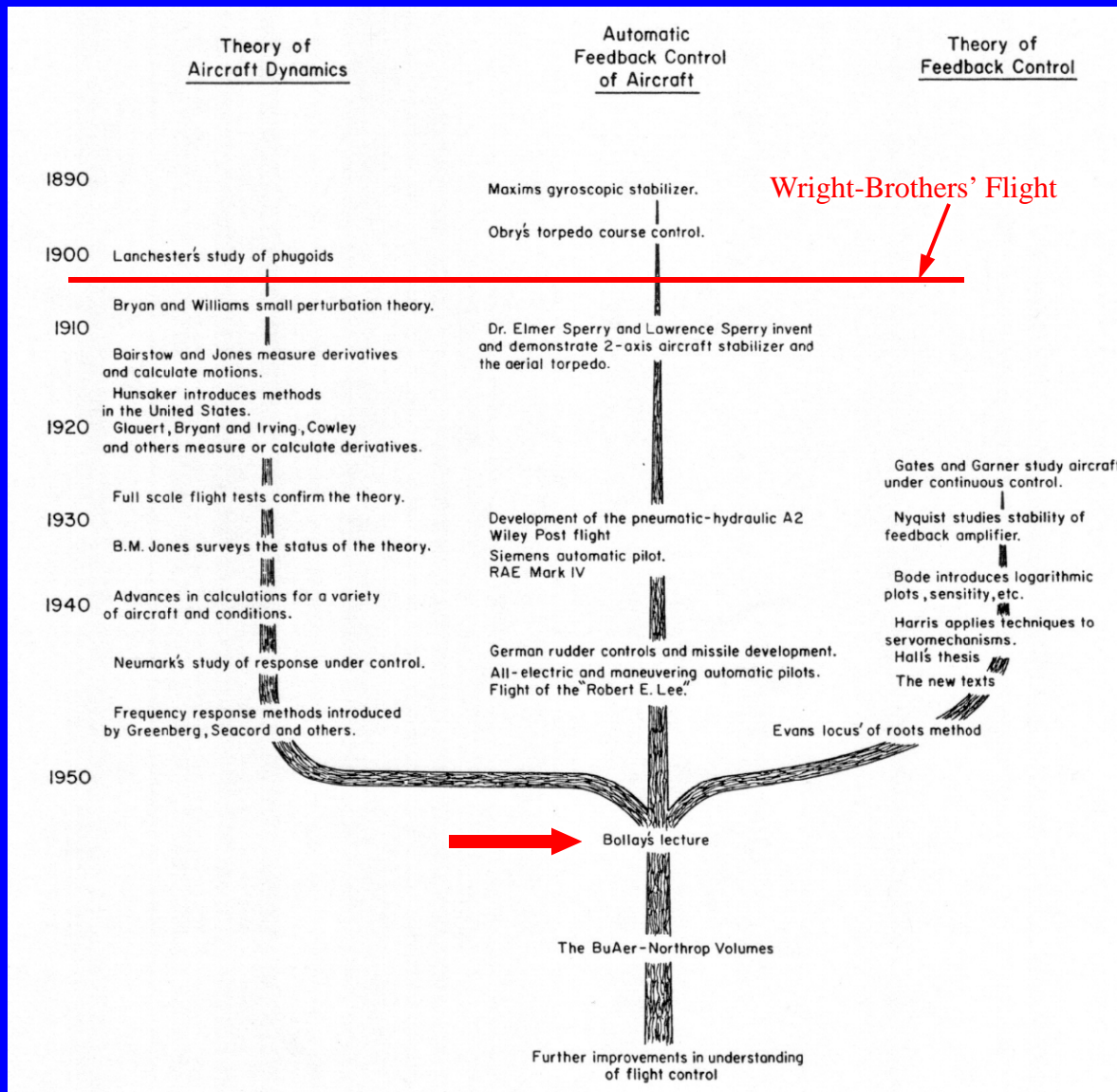
“The application of automatic control systems to aircraft promises to bring about the most important new advances in aeronautics in the future...The practicing aeronautical engineer will find it necessary to gain an understanding of these principles in order to design the optimum aircraft systems”

-William Bollay, “Aerodynamic Stability and Control,” *Journal of the Aeronautical Sciences*, 1951

“While the theoretical structure is well developed and practically applied in design, the actual selection of a design depends on a very large number of things which do not readily lend themselves to inclusion in, for example, a cost functional.”

-Duane McRuer and Dunstan Graham, “Eighty Years of Flight Control, Triumphs and Pitfalls of the Systems Approach,” *Journal of Guidance, Control and Dynamics*, 1981

The History of Flight Control



Functions of a Flight Control System

- Provide vehicle stability and controllability
- Reduce “effective” order of vehicle dynamics
- Adjust “effective” vehicle dynamic response
- Provide specified command-response relationships
- Reduce effects of unwanted inputs/disturbances
- Suppress effects of vehicle & component variations and uncertainties
- Improve linearity
- Modify or eliminate vehicle cross-coupling effects

→ Of increasing interest in controls community

Control System Design Techniques

- Ability of a control system design technique to provide a system with the functions just outlined is of obvious importance
- The ability to do so with *transparency*, i.e., to provide the control system engineer with insight as to how design decisions affect each functional requirement is equally vital
- A need to “bridge the gap” between theory and practice
 - QFT offers one approach
 - Frequency-domain, pseudo-sliding mode control (SMC) may offer another

Why Sliding-Mode Control Approach?

- Research Goal: Develop and demonstrate a design strategy for a MIMO flight control system which:
 - Applicable to the control of possibly unstable, high-performance aircraft
 - Robust to model uncertainty, smooth parameter variations, and sensor noise
 - Able to accommodate sudden, unknown, large system parameter changes due to failure events
 - Able to provide satisfactory handling qualities before failure and acceptable after failure
- Why this goal?

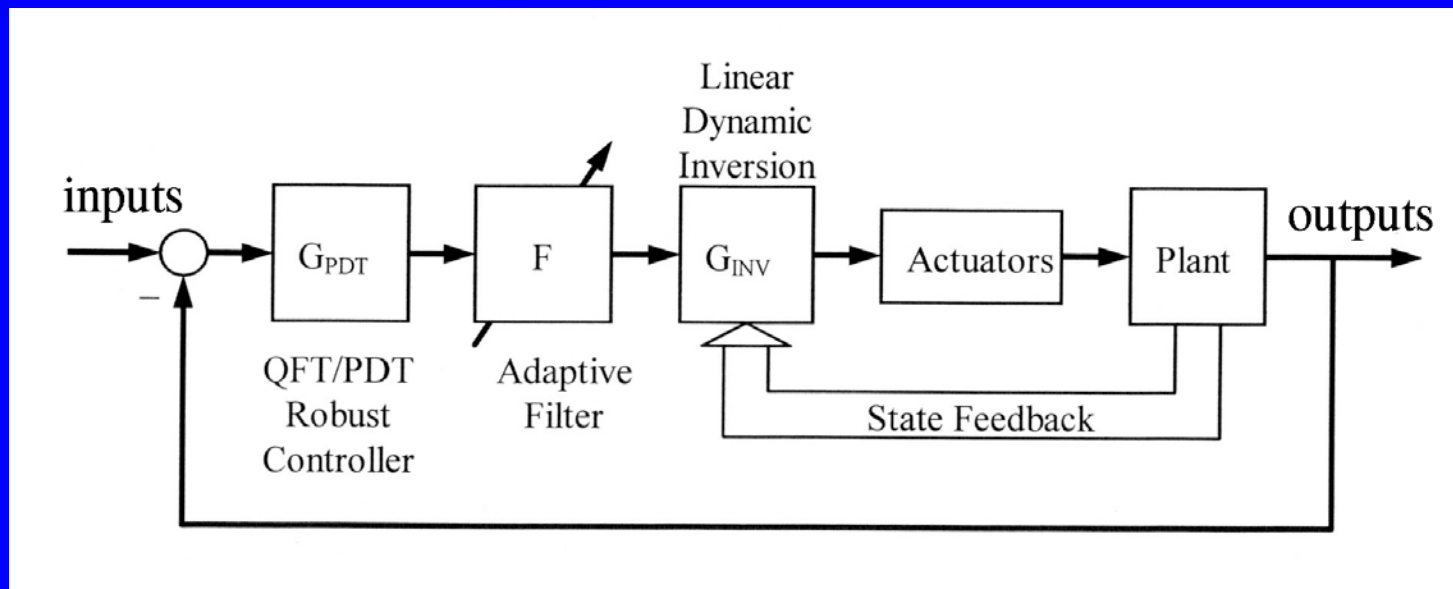
Why Sliding-Mode Control Approach?



because failure events do happen...

Frequency Domain Design via “Adaptive” QFT

Reduced-order, linear dynamic inversion coupled with diagonal QFT and adaptive module



Frequency Domain Design via “Adaptive” QFT

Siwakosit, W. and Hess, R. A. “Multi-Input/Multi-Output Reconfigurable Flight Control Design,” *Journal of Guidance, Control, and Dynamics*, Vol. 24, No. 6, 2001

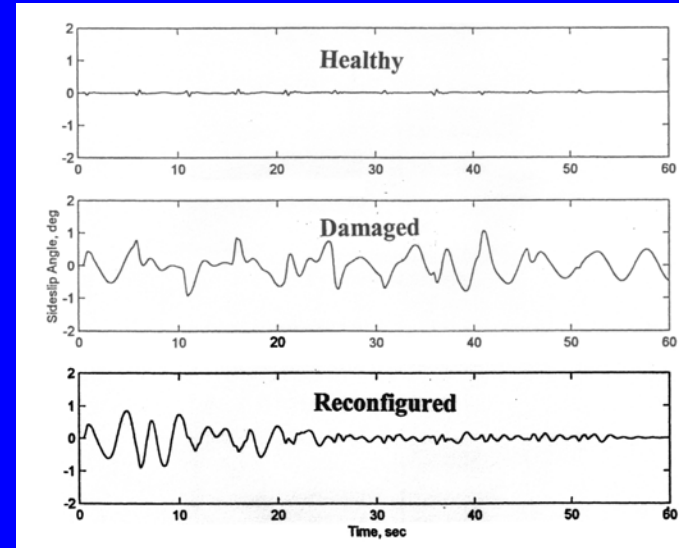
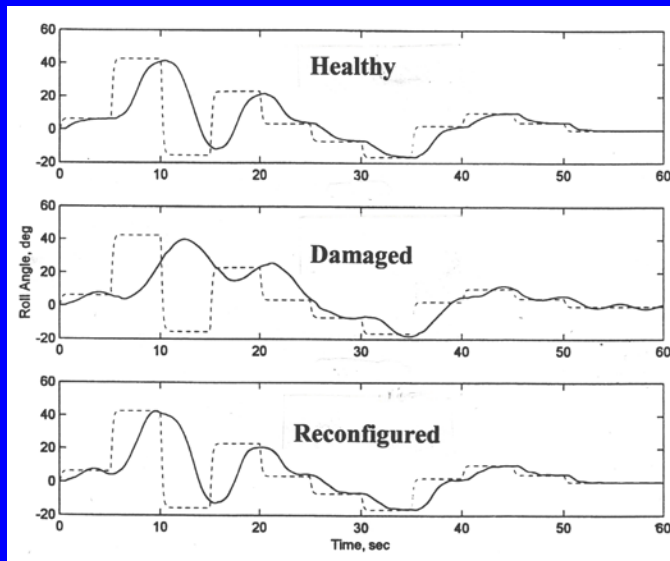
NASA HARV
High-Alpha Research Vehicle



Frequency Domain Design via “Adaptive” QFT

Frequency Domain Design via “Adaptive Quantitative Feedback Theory”

- HARV F-18 model; lateral directional control; Pilot model included
- Adaptive module implemented with filtered- ε algorithm
- Modeled vehicle “damage” @ “low-slow” flight condition: yaw thrust vector power reduced by 90%
- Took approx. 20 sec to converge



SMC Design Approach

Sliding Mode Control appeared as a promising alternative to “reconfigurable” architectures

- Extremely robust (invariant to matched uncertainty)
- No failure detection/isolation or system ID required
- No reconfiguration time -“instantaneous” adaptation

Formal Theory Overview

Consider the uncertain system with m inputs and n states described by:

$$\dot{\mathbf{x}}(t) = \mathbf{A}(\mathbf{x}, t) + \mathbf{B}(\mathbf{x}, t)\mathbf{u}(t) + \mathbf{E}\xi(\mathbf{x}, t)$$

ξ is unknown

Determine a switching surface σ and a variable structure control:

$$\mathbf{u}(\mathbf{x}, t) = \rho \operatorname{sgn}(\sigma)$$

Such that any state outside the surface is driven to the surface in finite time and remains on the surface for all subsequent time (called sliding mode)

Formal Theory Overview

Basic SMC properties:

- During the sliding mode, the trajectory dynamics are of lower order than that of original model
- While on the sliding surface, system dynamics governed solely by the parameters governing $\sigma = 0$ (insensitive to $\xi(t)$) and summarizes invariance inherent in SMC designs (so-called “matched uncertainty”)
- Existence of sliding mode requires stability of state trajectory relative to the sliding surface, leads to the *reachability condition*

$$\dot{\sigma}^T(t)\sigma(t) < 0$$

Formal Theory Overview

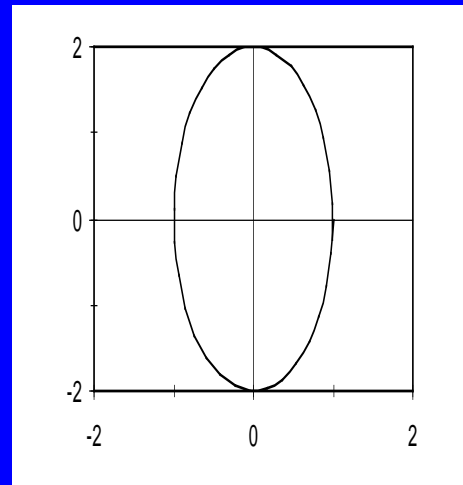
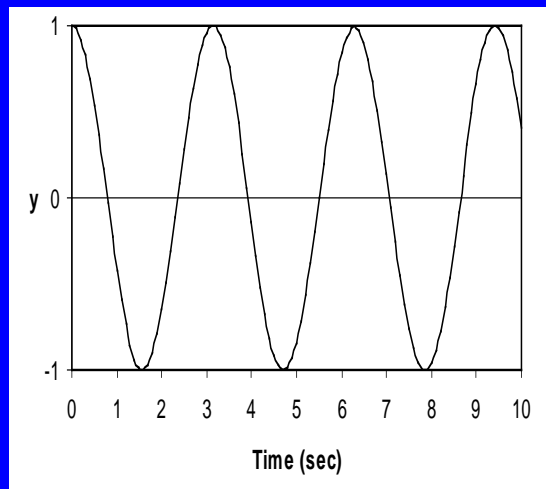
All SMC synthesis techniques contain two steps:

- Design the sliding surface(s) $\sigma = f(x)$
- Design the control law to reach the sliding mode in finite time $\rho = \text{sgn}(\sigma)$

An Example

Double Integrator With Proportional Control Law

$$\ddot{y}(t) = u(t) \quad u(t) = -k y(t)$$

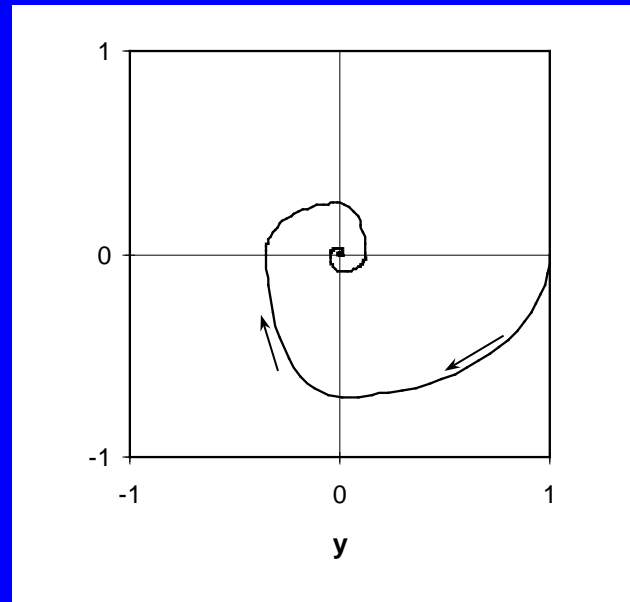
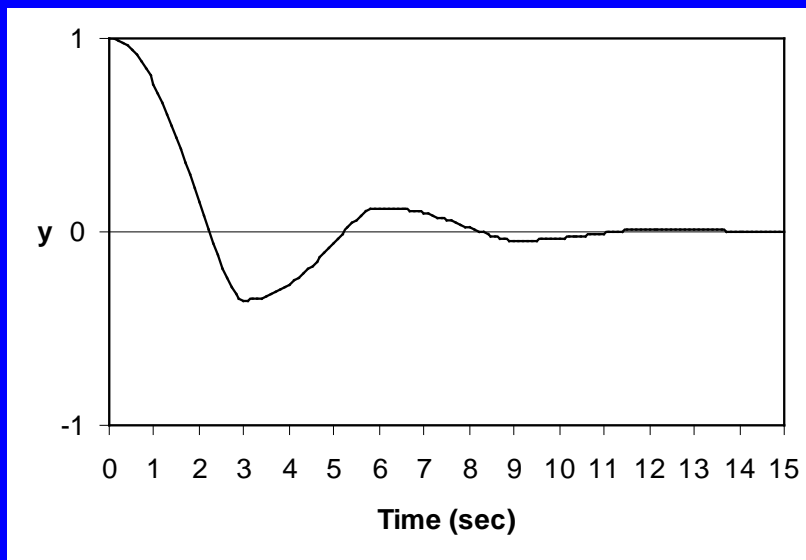


An Example

Double Integrator With Variable Structure Control Law

$$\ddot{y}(t) = u(t)$$

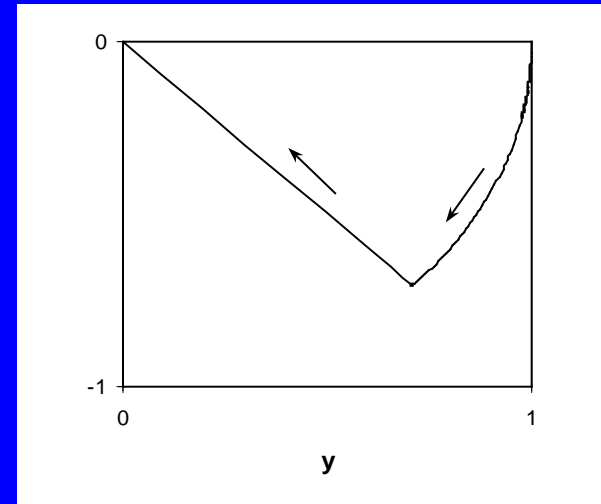
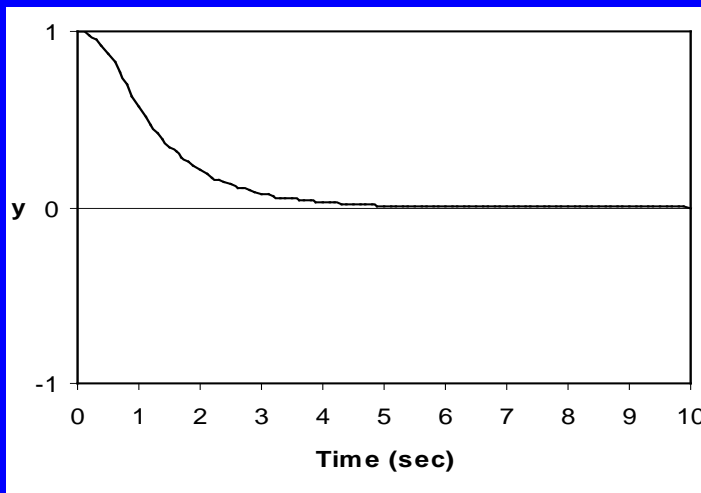
$$u(t) = \begin{cases} -k_1 y(t) & \text{if } y\dot{y} < 0 \\ -k_2 y(t) & \text{otherwise} \end{cases}$$



An Example

Double Integrator With Variable Structure Control Law

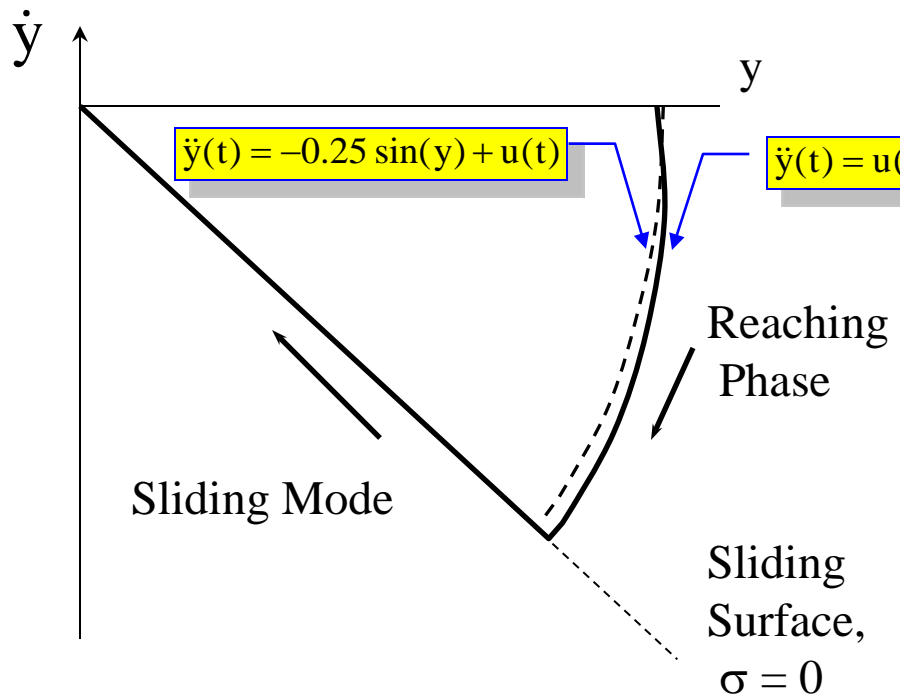
$$u(t) = \begin{cases} -1 & \text{if } \sigma(y, \dot{y}) > 0 \\ 1 & \text{if } \sigma(y, \dot{y}) < 0 \end{cases}$$



$$\sigma(y, \dot{y}) = m y + \dot{y}$$

An Example

Basic Concept



Sliding “Surface”

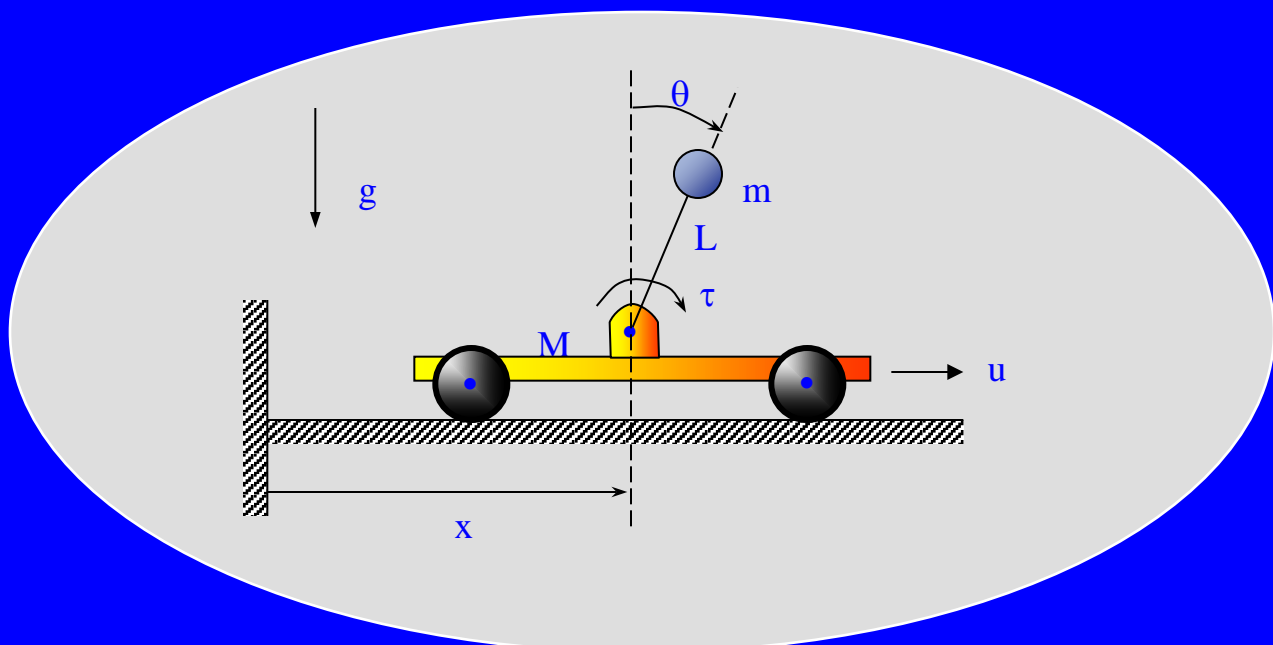
$$\sigma(y, \dot{y}) = m y + \dot{y}$$

Control Law

$$u(t) = \rho \times \begin{cases} -1 & \text{if } \sigma(y, \dot{y}) > 0 \\ 1 & \text{if } \sigma(y, \dot{y}) < 0 \end{cases}$$

An Example

Inverted Pendulum on a Translating Cart



An Example

Pendulum/Cart Equations of Motion

nonlinear
(used in simulation)



$$(M+m)\ddot{x} + F_x \dot{x} + (mL\cos\theta)\ddot{\theta} - mL\dot{\theta}^2 \sin\theta = u$$

$$J\ddot{\theta} + F_\theta \dot{\theta} - mLg \sin\theta + (mL\cos\theta)\ddot{x} = \tau$$

linear
(used in design)

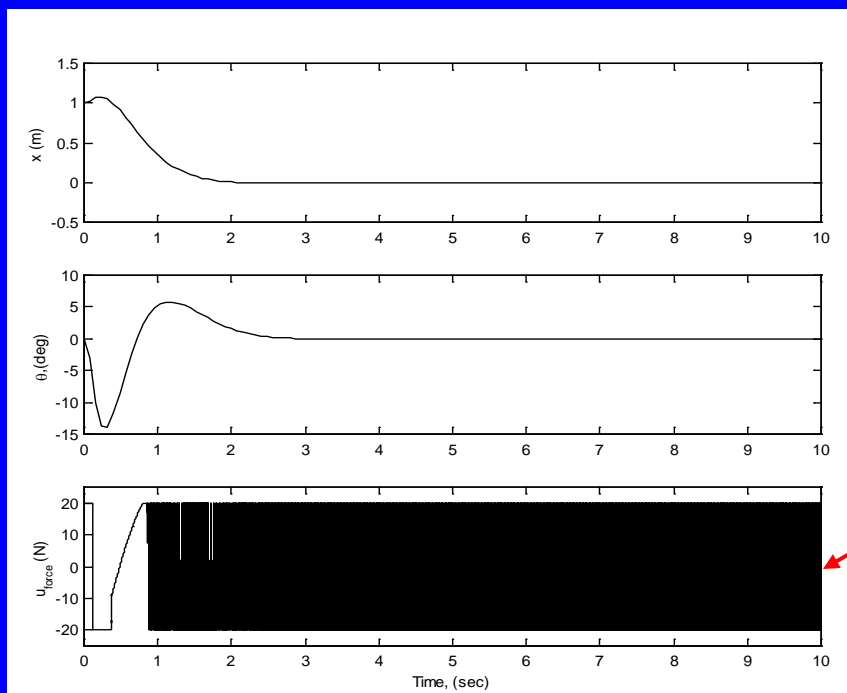


$$\begin{bmatrix} \dot{x}_1 \\ \dot{x}_2 \\ \dot{x}_3 \\ \dot{x}_4 \end{bmatrix} = \begin{bmatrix} 0 & 0 & 1 & 0 \\ 0 & 0 & 0 & 1 \\ 0 & \frac{-m^2 L^2 g}{J(M+m) - m^2 L^2} & \frac{-J F_x}{J(M+m) - m^2 L^2} & \frac{m L F_\theta}{J(M+m) - m^2 L^2} \\ 0 & \frac{(M+m)mLg}{J(M+m) - m^2 L^2} & \frac{m L F_x}{J(M+m) - m^2 L^2} & \frac{-(M+m)F_\theta}{J(M+m) - m^2 L^2} \end{bmatrix} \begin{bmatrix} x_1 \\ x_2 \\ x_3 \\ x_4 \end{bmatrix}$$

$$+ \begin{bmatrix} 0 & 0 \\ 0 & 0 \\ \frac{J}{J(M+m) - m^2 L^2} & \frac{-mL}{J(M+m) - m^2 L^2} \\ \frac{-mL}{J(M+m) - m^2 L^2} & \frac{(M+m)}{J(M+m) - m^2 L^2} \end{bmatrix} \begin{bmatrix} u \\ \tau \end{bmatrix}$$

An Example

$(\tau = 0)$ Manifold from Regular Form
nonlinear simulation



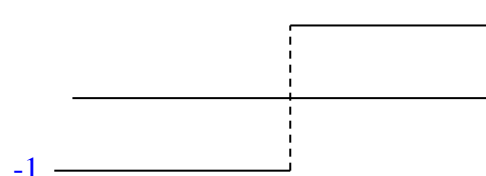
$$u = 20 \operatorname{sgn}(\sigma)$$

infinite-frequency
switching

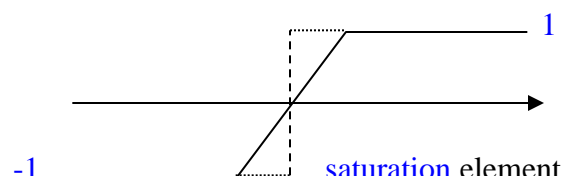
Achieving Continuous Control

Methods to achieve continuous control

- Second-order sliding mode
- Boundary layers



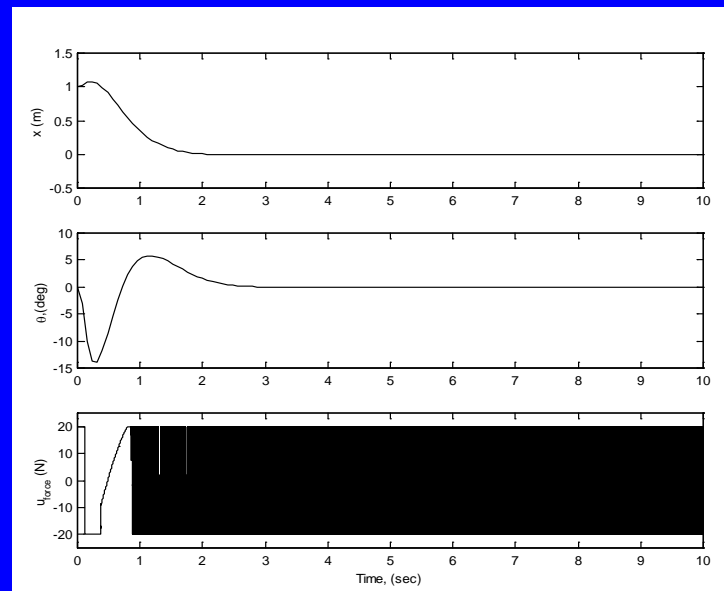
$\text{sgn}(\sigma)$



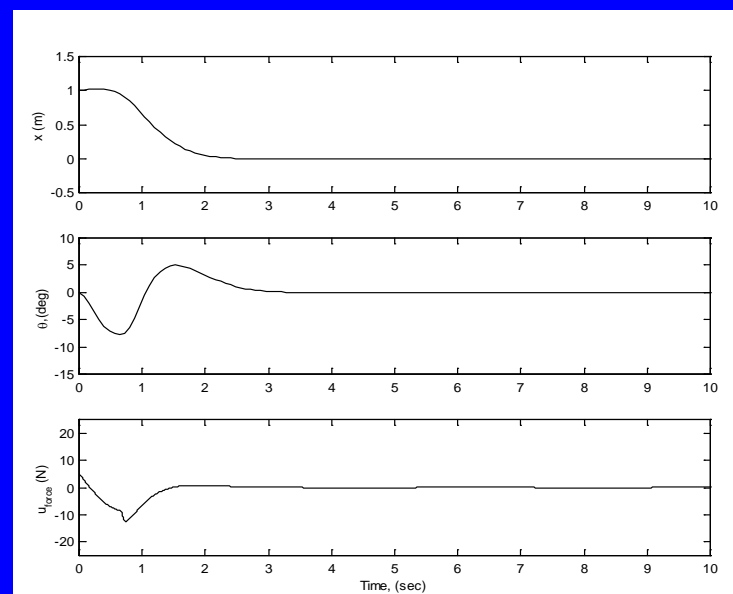
$\text{sat}\left(\frac{\sigma}{\varepsilon}\right)$

Achieving Continuous Control

without boundary layer
sliding mode control

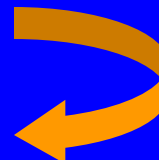


with boundary layer
pseudo-sliding mode control



SMC Design for Multi-Input, Multi-Output Systems

- All SMC synthesis techniques contain two steps:
 - Design the sliding surface(s) $\sigma = f(x)$
 - Design the control law to reach the sliding mode in finite time $\rho = \text{sgn}(\sigma)$
- Many approaches for MIMO systems
 - Square feedback linearizable systems
 - Frequency domain loop shaping



SMC Design for Multi-Input, Multi-Output Systems

The two major assumptions are involved in this approach are:

- (a) the system is square, i.e., an equal number of inputs and outputs, and
- (b) the system is feedback linearizable, i.e., no transmission zeros lie in the right half plane and uncontrollable states must be stable.

If the system in question meets these criteria, it is possible to decouple the outputs with the given inputs. This transforms a multi-input, multi-output (MIMO) design into m single-input, single-output (SISO) designs, where m is the number of inputs or outputs.

SMC Design for Multi-Input, Multi-Output Systems

Consider a non-linear, square MIMO system

$$\dot{\mathbf{x}} = \mathbf{A}(\mathbf{x}) + \mathbf{B}(\mathbf{x})\mathbf{u}$$

$$\mathbf{y} = \mathbf{C}(\mathbf{x})$$

where $\mathbf{x} \in \Re^n$, $\mathbf{y} \in \Re^m$, $\mathbf{u} \in \Re^m$. Assume the functions $\mathbf{A}(\mathbf{x})$, $\mathbf{C}(\mathbf{x})$ and columns $b_i(\mathbf{x})$ of the matrix $\mathbf{B}(\mathbf{x}) \in \Re^{n \times m}$ are smooth vector fields. Further, assume the system is completely linearizable in a reasonable domain $\mathbf{x} \in \Gamma$. The control system will be designed to track a real-time reference profile, $\mathbf{y}_r(t)$. First, m independent sliding surfaces or manifolds are created.

$$\sigma_i = e_i^{(r_i-1)} + c_{i,r_i-2}e_i^{(r_i-2)} + \dots + c_{i,1}e_i^{(1)} + c_{i,0}e_i \quad \forall i = 1, m$$

SMC Design for Multi-Input, Multi-Output Systems

$$\sigma_i = e_i^{(r_i-1)} + c_{i,r_i-2}e_i^{(r_i-2)} + \dots + c_{i,1}e_i^{(1)} + c_{i,0}e_i \quad \forall i = 1, m$$

$$e_i = y_{r,i}(t) - y_i(t), \quad e_i^{(j)} = \frac{d^j e_i}{dt^j}$$

Note that these have orders exactly one less than the relative order r_i for the corresponding state variable, where relative order refers to the order of the derivative of y_i necessary to ensure that a term containing an element of \mathbf{u} appears. The coefficients $c_{i,j}$ are design parameters which can be chosen in a number of ways, e.g., frequency-domain loop shaping

The control law that can be used is

$$u_i = \rho_i \operatorname{sgn}(\sigma_i)$$

SMC Design for Multi-Input, Multi-Output Systems

In order to prove system stability one can refer to scalar representation of

$$\dot{\sigma}^T(t)\sigma(t) < 0$$

The parameter ρ_i will appear in the expression for $\dot{\sigma}_i$

Determine the minimum ρ_i that will provide global attractiveness to the sliding surface in finite time, i.e., that ensures that

$$\dot{\sigma}_i \sigma_i < 0$$

However, in systems in which a human agent is active in outer-loop control, such in piloted aircraft, this approach is problematic, as expressions for will be an unknown function of the pilot's control inputs

SMC Design for Multi-Input, Multi-Output Systems

With

$$\sigma_i = e_i^{(r_i-1)} + c_{i,r_i-2}e_i^{(r_i-2)} + \dots + c_{i,1}e_i^{(1)} + c_{i,0}e_i \quad \forall i = 1, m$$

and

$$u_i = \rho_i \text{sat}\left(\frac{\sigma_i}{\varepsilon_i}\right)$$

At a sufficiently high frequency, the loop transmission will look like

$$L(s) = K/s$$

And excellent robust control performance can be obtained

Loop Shaping

$$\sigma = c_1 \dot{e} + c_0 e + c_{-1} \int e dt$$

an SMC with a boundary layer

$$u = \rho \text{sat}\left(\frac{\sigma}{\varepsilon}\right)$$

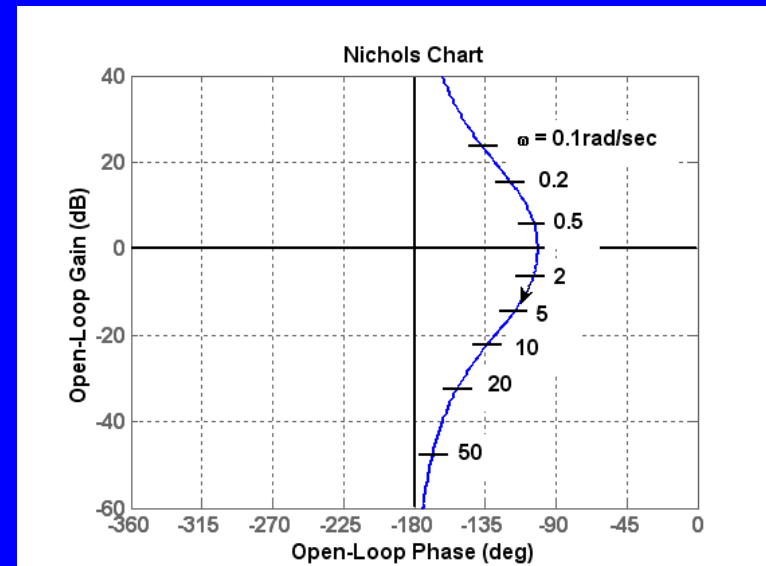
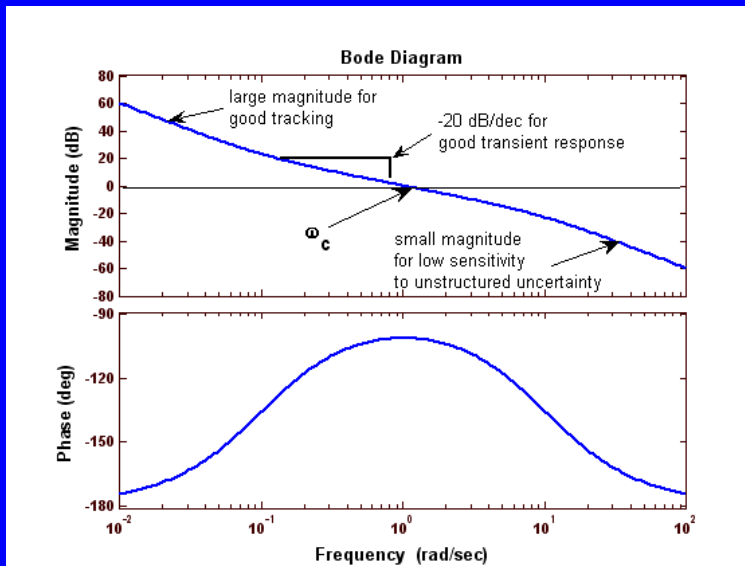
looks like a linear PID controller

$$u(s) = \frac{\rho}{\varepsilon} \sigma = \frac{\rho}{\varepsilon} \left(c_1 s + c_0 + \frac{c_{-1}}{s} \right) e(s)$$

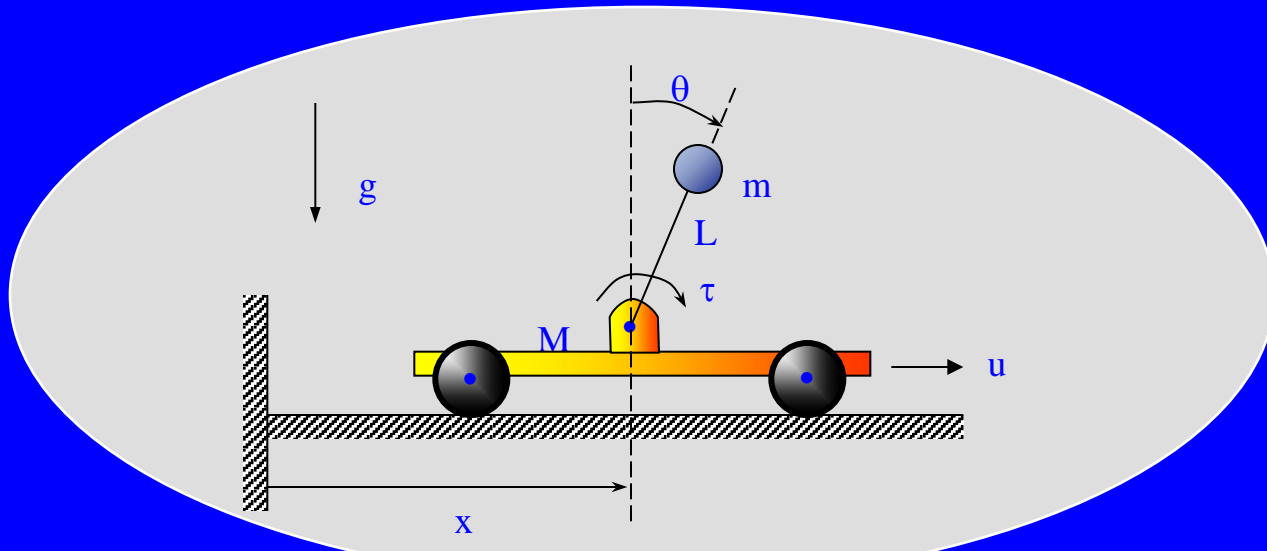
Can use traditional frequency domain loop shaping techniques to define the sliding manifold

The ‘Fundamental Rule of Thumb’ in Frequency-Domain Design

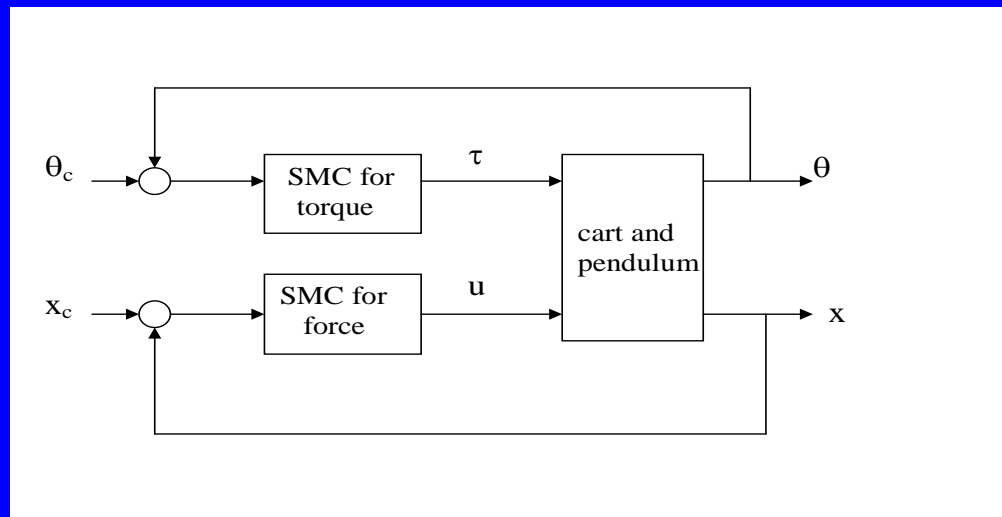
Find or create a fair stretch of -20 dB/dec slope for the amplitude ratio for the loop transmission $L(j\omega)$, and then make it the crossover frequency region by putting the 0 dB line through it. Choose the crossover frequency (ω_c) as the desired closed-loop bandwidth. Ensure that for frequencies will below ω_c that $|L(j\omega)| \gg 1.0$ and for frequencies will above ω_c that $|L(j\omega)| \ll 1.0$



An Example



Now consider u and τ controller inputs



An Example

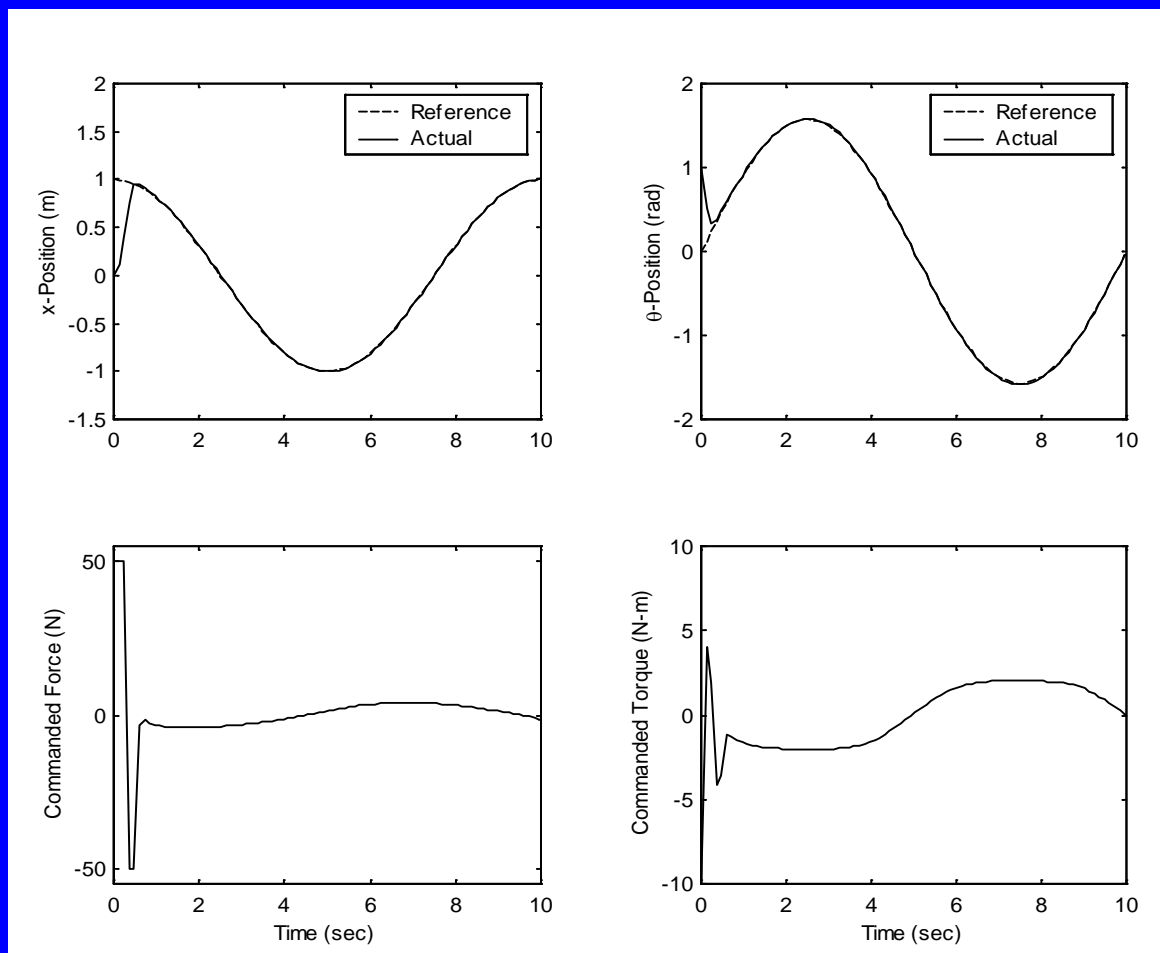
sliding manifolds:

$$\sigma_x = (\dot{x}_c - \dot{x}) + 10(x_c - x) \quad \sigma_\theta = (\dot{\theta}_c - \dot{\theta}) + 10(\theta_c - \theta)$$

SMC control laws:

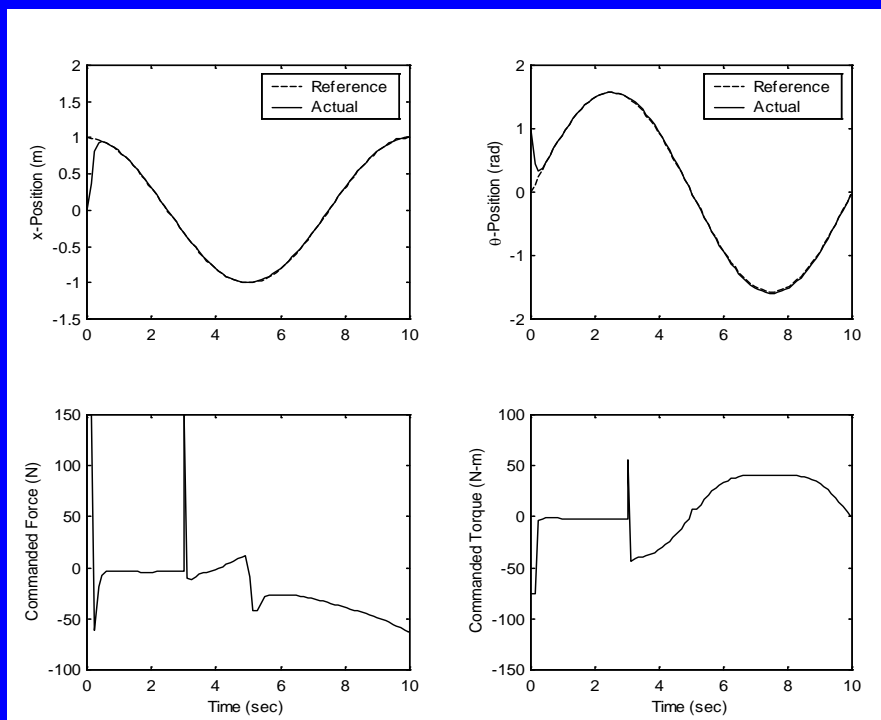
$$u = 50 \operatorname{sat}\left(\frac{\sigma_x}{0.4}\right) \quad \tau = 10 \operatorname{sat}\left(\frac{\sigma_\theta}{0.4}\right)$$

An Example



An Example

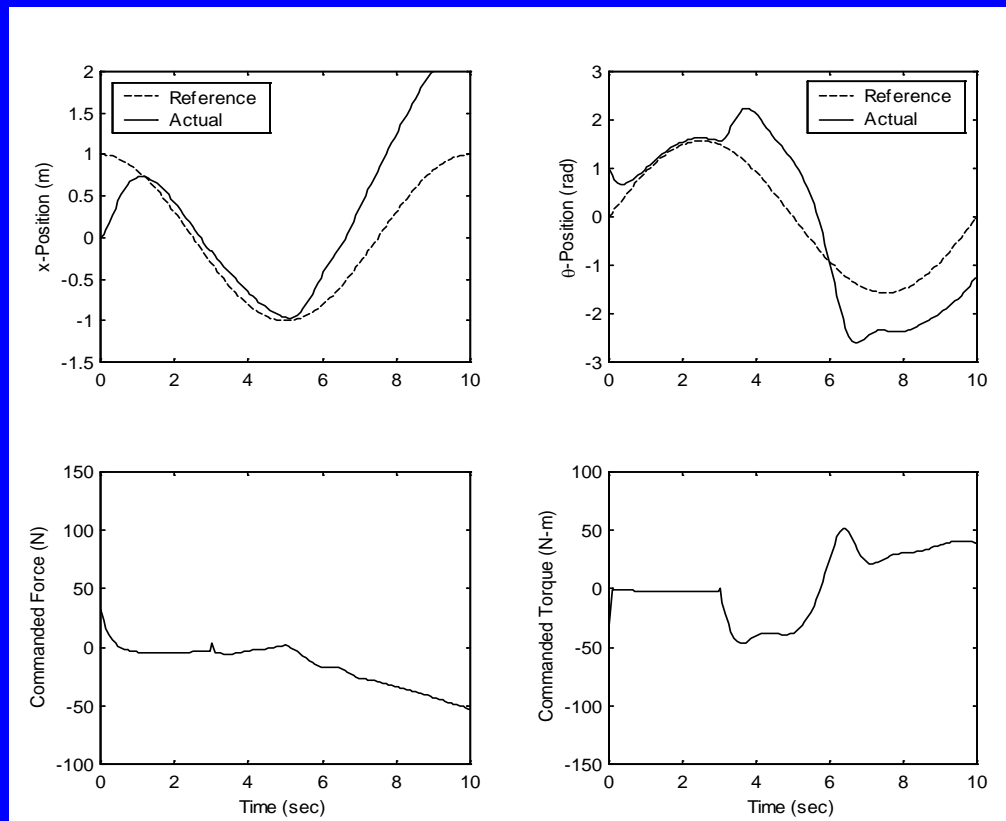
SMC Decoupled Feedback Linearization with system failure @ $t = 3$ sec + control bias @ $t = 5$ sec



Parameter	Nominal Value	Value after "Failure"
Cart Mass, M	3.0 kg	30.0 kg
Pendulum Mass, m	0.50 kg	5.0 kg
Rod Length, L	0.4 m	0.8 m
Linear Friction Coef, F_x	6.0 kg/s	25.0 kg/s
Angular Friction Coef, F_θ	0.005 kg·m ²	0.05 kg·m ²

An Example

LQR Design with system failure @ $t = 3$ sec + control bias @ $t = 5$ sec



SMC Design for Multi-Input, Multi-Output Systems

- Parasitic dynamics can compromise the design of SMC systems
- In aerospace applications, parasitic dynamics are typically associated with actuators
- Addition of first-order actuators $10/(s+10)$ destabilizes cart/pendulum!!

Dealing With Parasitic Dynamics

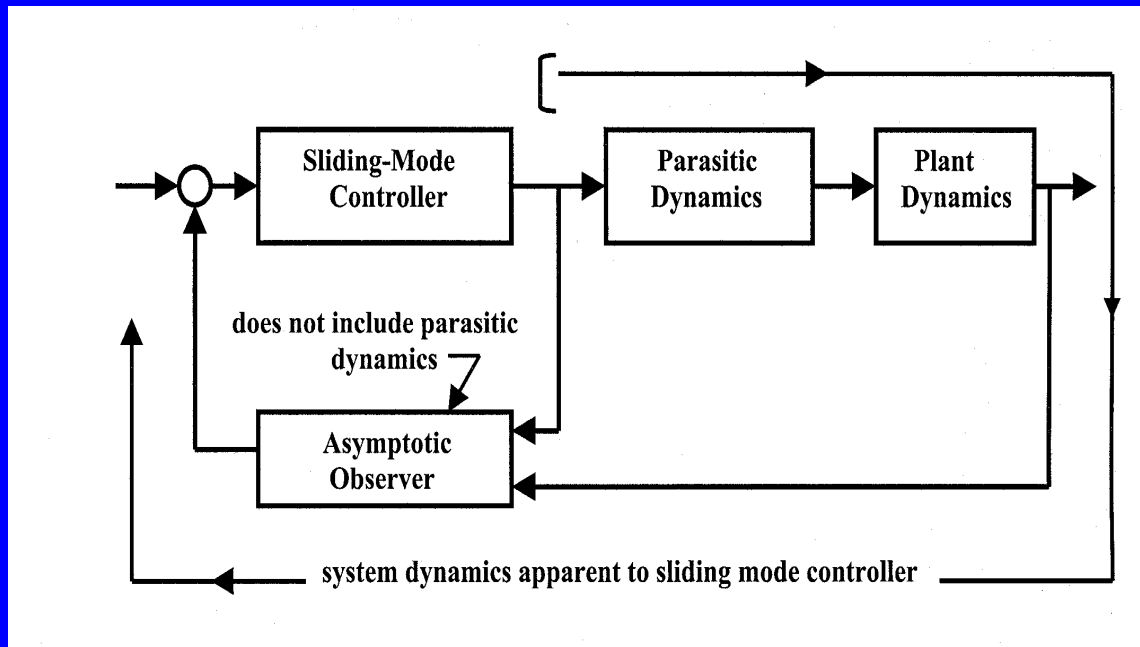
Some Potential Solutions

- Include the dynamics in plant model
- Dynamic Boundary Layer Control
- Observer-Based SMC 

Observer-Based SMC

$$\dot{\hat{x}} = \mathbf{A}\hat{x} + \mathbf{B}u + \mathbf{K}_e(y - \mathbf{C}\hat{x})$$

Observer “hides” the parasitic dynamics from SMC system



Observer-Based SMC

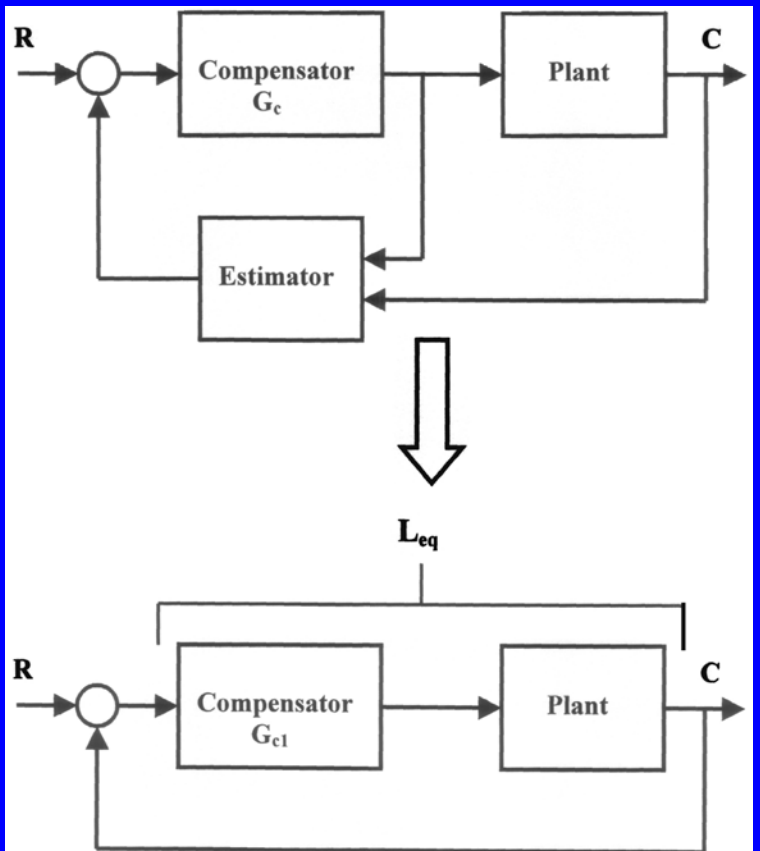
The eigenvalues can be shown to affect SMC performance in the following manner:

- Large observer eigenvalues increase the robustness of the SMC design to variations in vehicle characteristics but also increase the susceptibility of the design to the deleterious effects of unmodelled parasitic dynamics.
- Small observer eigenvalues decrease the robustness of the SMC design to variations in vehicle characteristics, but also decreases the susceptibility of the design to the effects of unmodelled parasitic dynamics.
- Proposed method provides useful design tool
- Can use multiple observers for MIMO applications

Observer-Based SMC

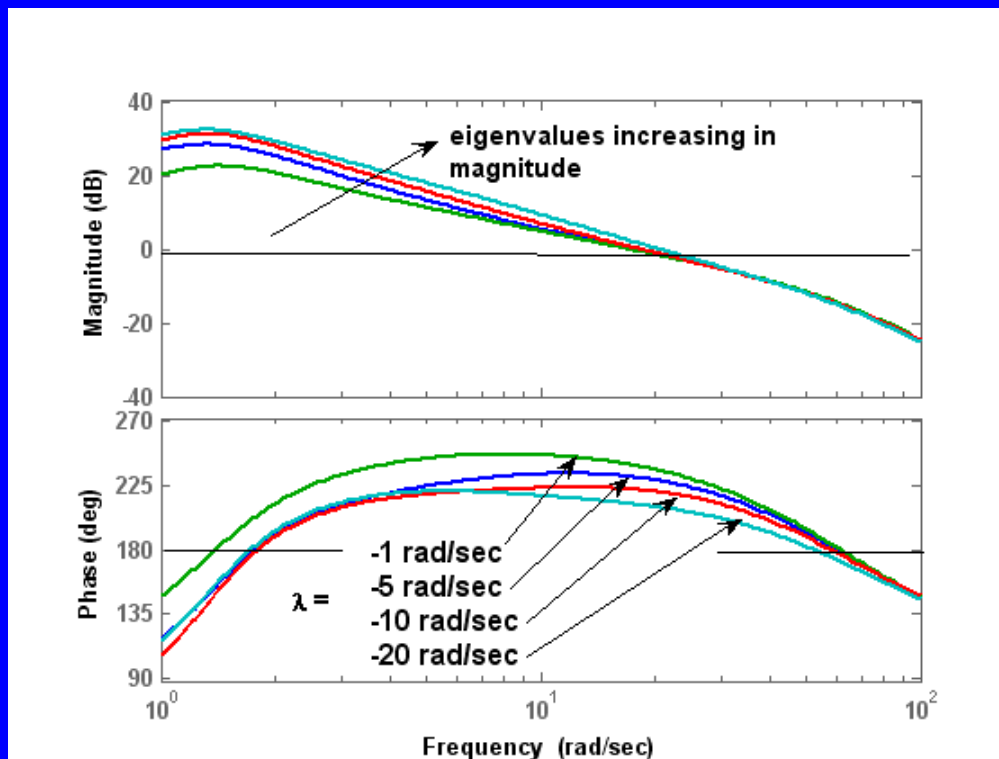
Selecting Observer Eigenvalues
(consider all real and nearly equal)

- Form “equivalent unity-feedback loop transmission L_{eq}
- Create Bode plot of L_{eq} for different eigenvalues sets
- Select eigenvalues based upon a trade-off between low-freq magnitude and stability margins.



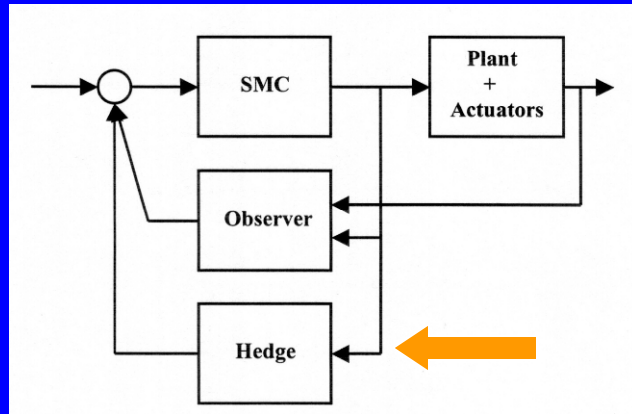
Observer-Based SMC

Selecting observer eigenvalues
UAV example



$$\lambda_i = -5 \text{ rad/sec} \text{ chosen}$$

Reference Model Hedging



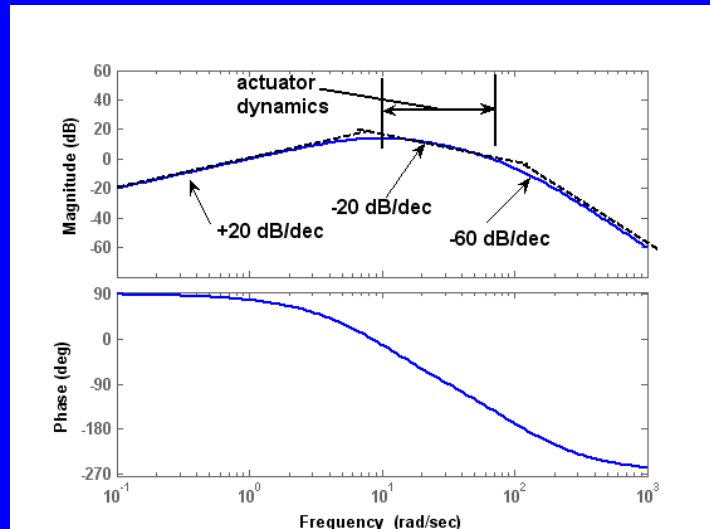
- Reference model hedging is equivalent to a filter in parallel with the observer – goal similar to Loop Transfer Recovery
 - Provides additional tool for shaping the feedback signal
 - Further diminishes effects of actuator dynamics
 - Allow use of large observer eigenvalues – improves robustness

Reference Model Hedging

Hedge Dynamics = $G_{\text{hedge}} = G_h G_f$

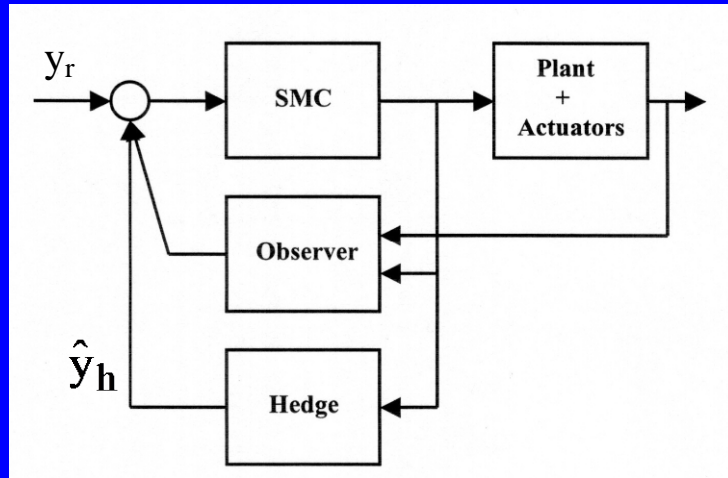
$$G_h = \frac{a_0}{(s^{r_i+1} + a_{r_i}s^{r_i} + \dots + a_0)}$$

$$G_f = \frac{s}{s+b}$$



G_{hedge} is created so that the magnitude portion of its Bode diagram exhibits the following characteristics: $+20 \text{ dB/dec}$ slope at low frequencies, $-20r_1 \text{ dB/dec}$ slope at frequencies where the (neglected) actuator dynamics distort the magnitude curve of \hat{y}_h / y_r (r_1 = the relative order of system without parasitic dynamics) and, $-20(r_1+1) \text{ dB/dec}$ slope at high frequencies.

Reference Model Hedging



The gain K_h is then varied until the transfer function \hat{y}_h / y_r closely approximates that for the vehicle without parasitic dynamics while employing as large as eigenvalues as possible in the corresponding observer. The similarity between this generalized hedging and loop transfer recovery as utilized in linear quadratic gaussian control designs should be noted.

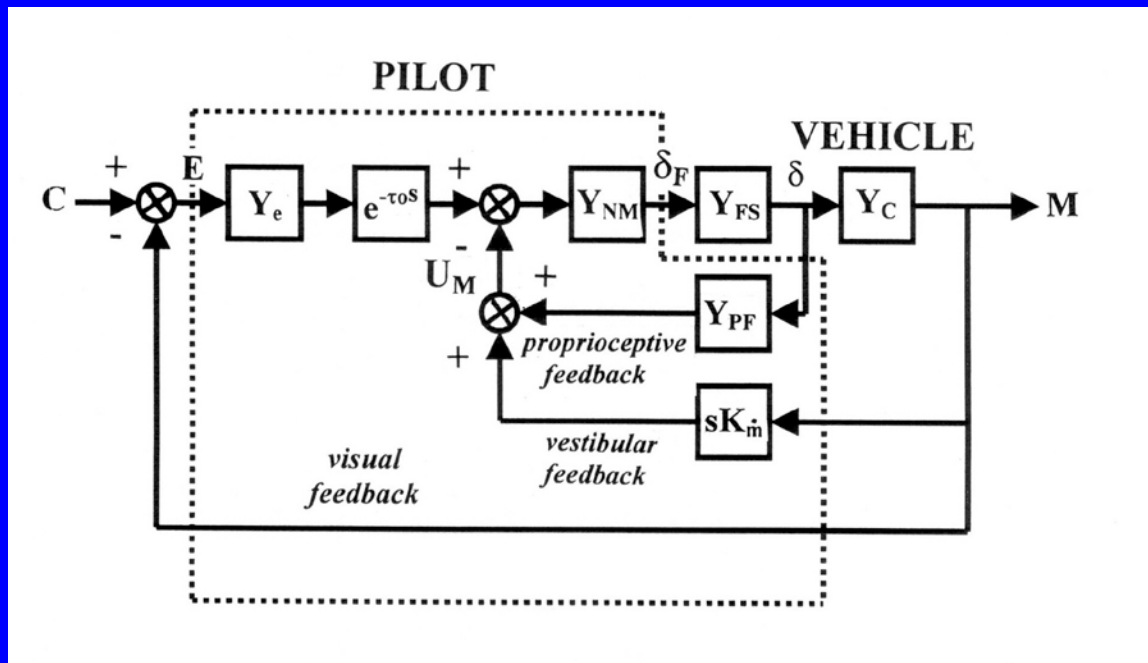
SMC Design Procedure

- (1) Obtain vehicle model (neglect actuators)
- (2) Define reference model (handling qualities constraints)
- (3) Define feedback structure (square)
- (4) Define sliding manifold (frequency domain technique)
- (5) Validate sliding mode behavior
- (6) Include SMC boundary layer
- (7) Introduce unmodeled actuator dynamics
- (8) Design observer(s) and hedge model
- (9) If necessary, schedule observers with flight condition
- (10) Validate (Bode plots, time history, handling qualities predictions)

Control Theoretic Human Pilot Models

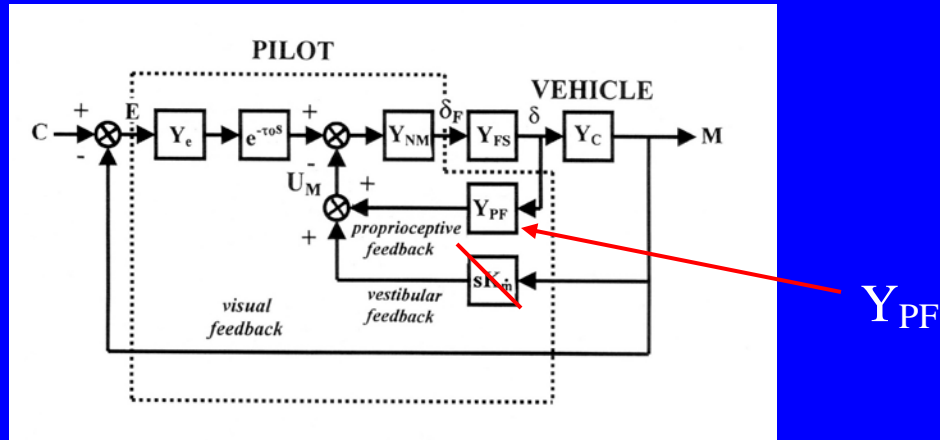
- The evaluation of flight control laws for piloted aircraft inevitably include performance and handling qualities evaluations.
- When applied to systems that will be subject to manual control, the results of the synthesis procedure just outlined should also be subject to a pilot/vehicle analysis
- In an analytical framework, this means relying upon mathematical models of the human pilot. The pilot model to be discussed here is the control-theoretic representation known as the Structural Model

Control Theoretic Human Pilot Models



Structural Model of Human Pilot

Structural Model of Human Pilot

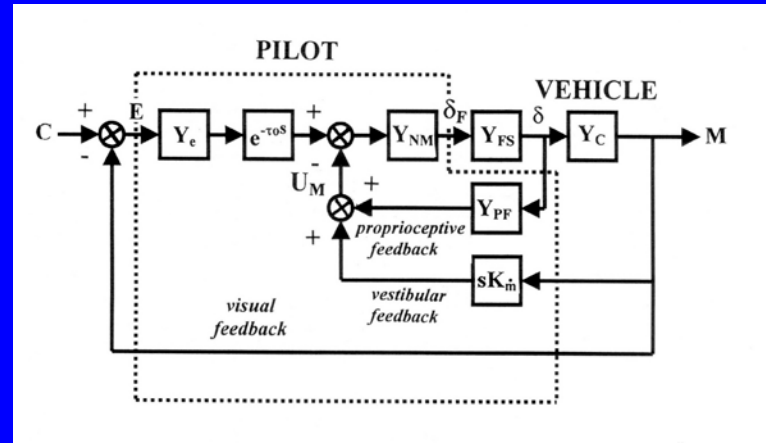


For the great majority of applications, the proprioceptive feedback element Y_{PF} takes one of the following forms:

$$Y_{PF} = K(s + a), \quad K \quad \text{or} \quad K / (s + a)$$

with the particular dependent upon the form of the vehicle dynamics (including flight control system) in the region of the open-loop crossover selected as 2.0 rad/sec.

Structural Model of Human Pilot



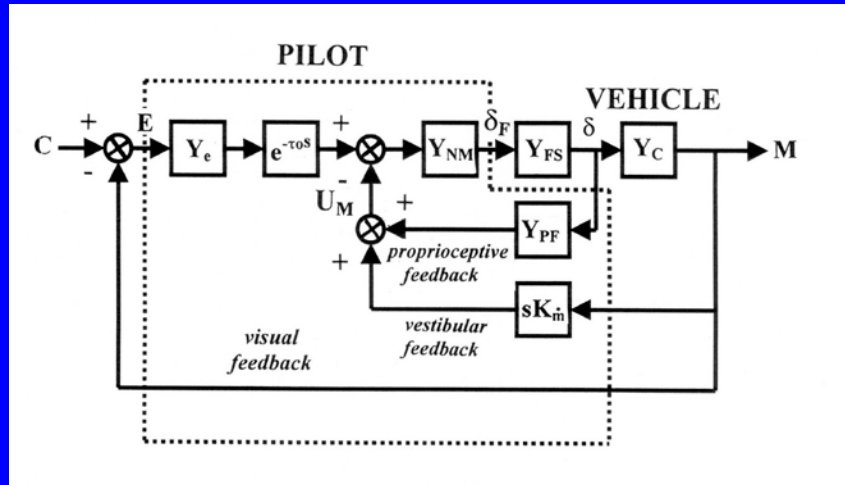
- With $Y_c(s)$ representing the transfer function of the “effective” vehicle (aircraft + flight control system) for $\omega \approx \omega_c = 2$ rad/sec and K_1 arbitrary

$$\frac{Y_c(j\omega)}{Y_{PF}(j\omega)} \approx \frac{K_1}{(j\omega)}$$

- The element Y_{NM} is a simplified model of the neuromuscular system in the pilot’s limb that is effecting control and is represented by

$$Y_{NM}(s) = \frac{10^2}{(s^2 + 14.14s + 10^2)}$$

Structural Model of Human Pilot

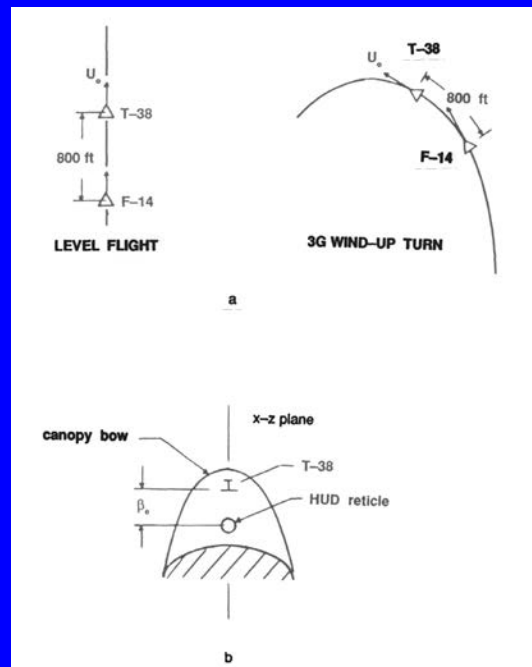
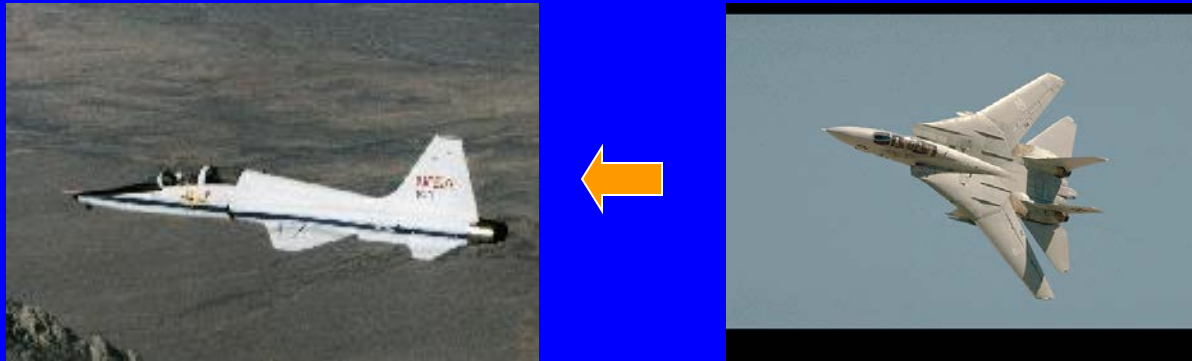


- The element Y_{FS} represents the (linear) dynamics of the force/feel system of the cockpit inceptor in question.
- Finally, the element Y_e is selected as

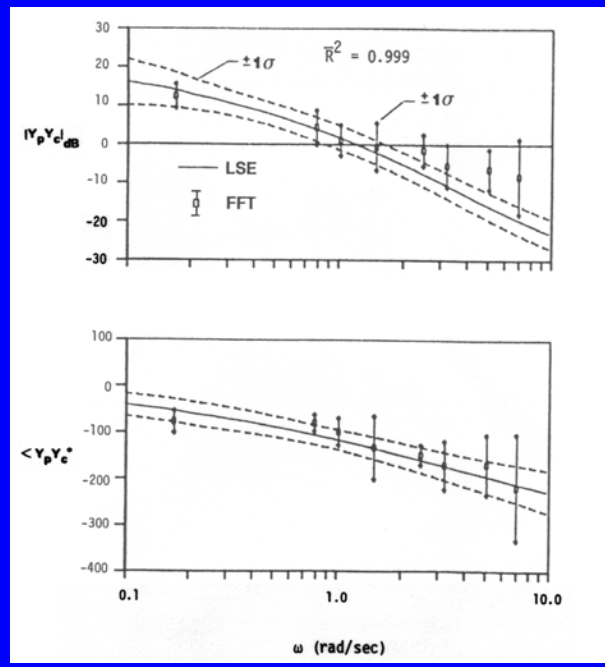
$$Y_e = \frac{K_e [s + (\omega_c / 2)]}{s}$$

- K in $Y_{PF} = K(s + a)$, K or $K/(s + a)$ selected to give minimum damping ratio of 0.15 in inner-most loop of pilot model

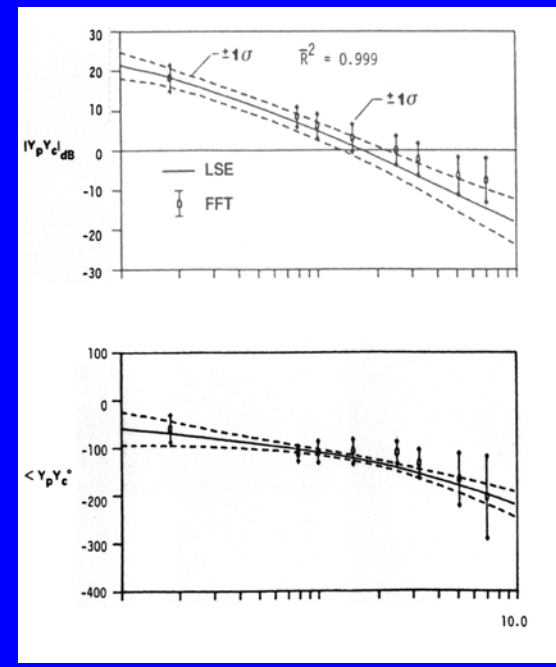
Measuring the Human Operator “Transfer Function”



- (a) Tail-chase task geometry,
- (b) F-14 head-up display

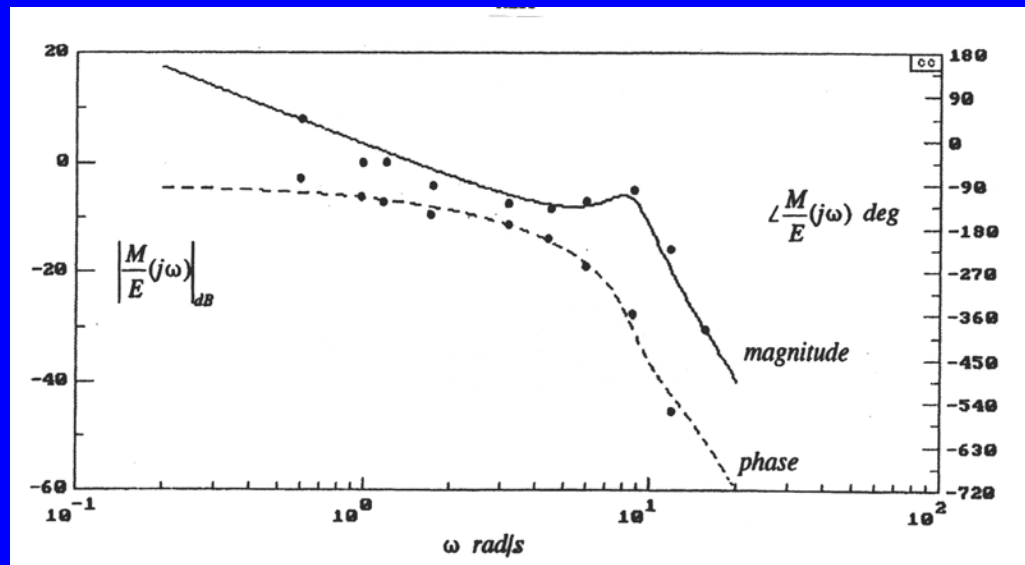


Measured loop transmission from level-flight



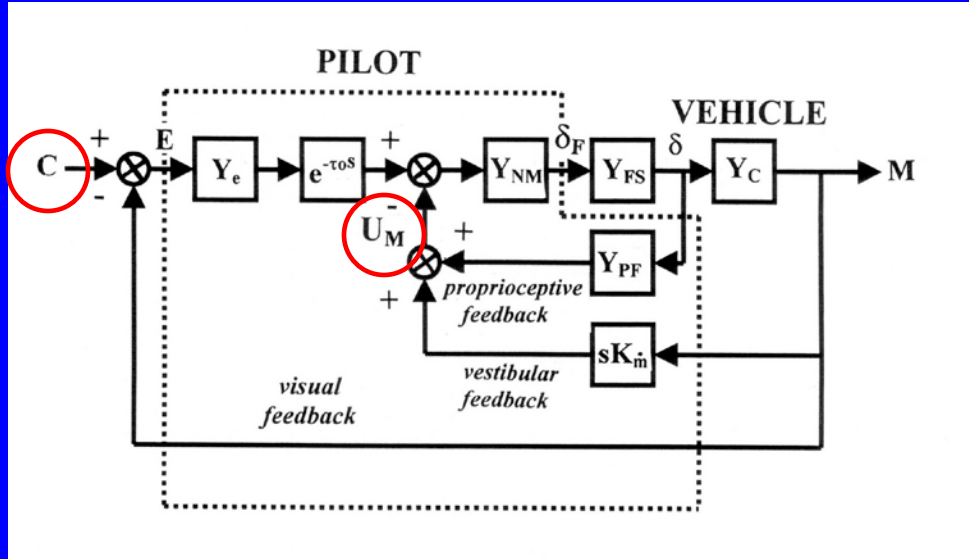
Measured loop transmission from wind-up turn

Structural Model of Human Pilot



In-flight measured (points) and pilot-model generated (solid lines) loop transmissions

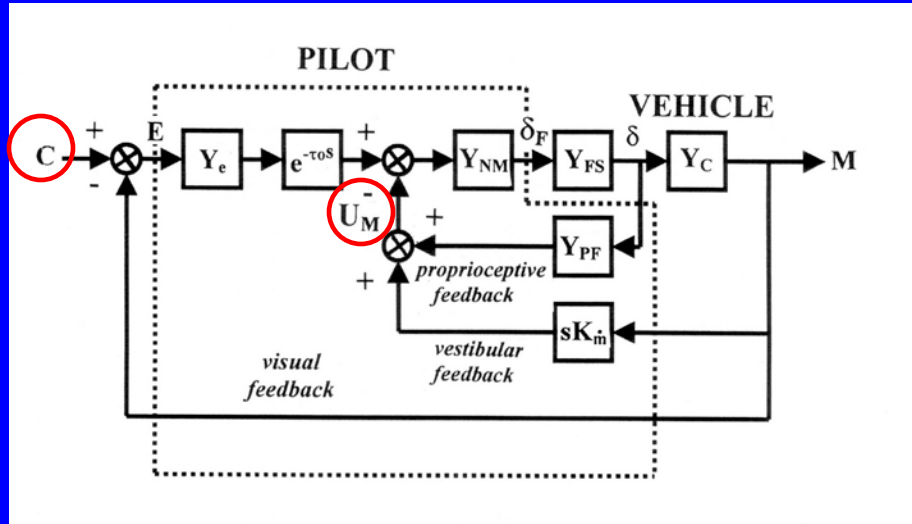
Analytical Handling Qualities Assessment



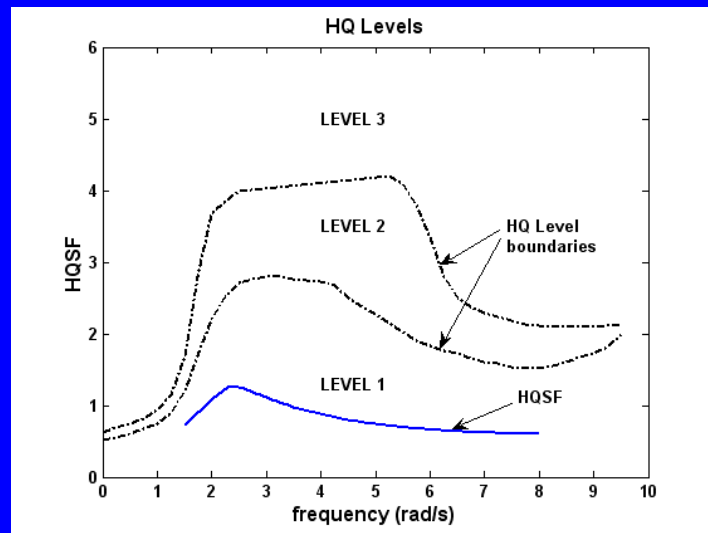
With the pilot model selected as described in the preceding section, a Handling Qualities Sensitivity Function (HQSF) can be defined as

$$HQSF = \frac{1}{|K_e|} \left| \frac{U_M(j\omega)}{C} \right|$$

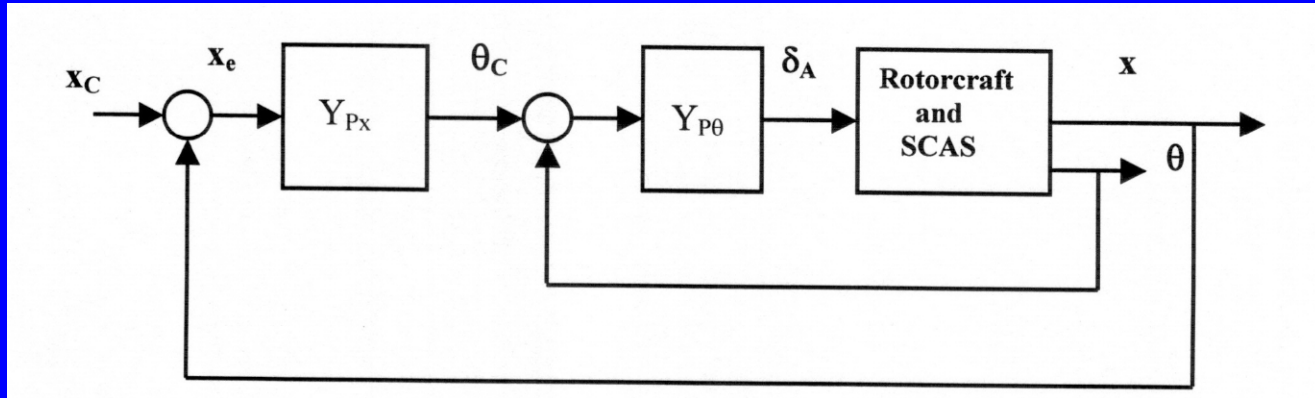
Analytical Handling Qualities Assessment



$$HQSF = \frac{1}{|K_e|} \left| \frac{U_M}{C} (j\omega) \right|$$



Pilot Model Formulation – Multi-Axis, Multi-Loop



- A multi-loop application of the pilot modelling procedure, here for a hovering rotorcraft.
- $Y_{P\theta}$ represents the Structural Pilot Model
- Y_{Px} represents the pilot equalization activity in the outer, position loop.
- Outer loop pilot models such as Y_{Px} are typically very simple in form, chosen so that the transfer function

$$\frac{X}{X_e}(s) \approx \frac{\omega_{c\theta}/3}{s}$$

A Frequency-Domain Based “Structural” Pilot Model

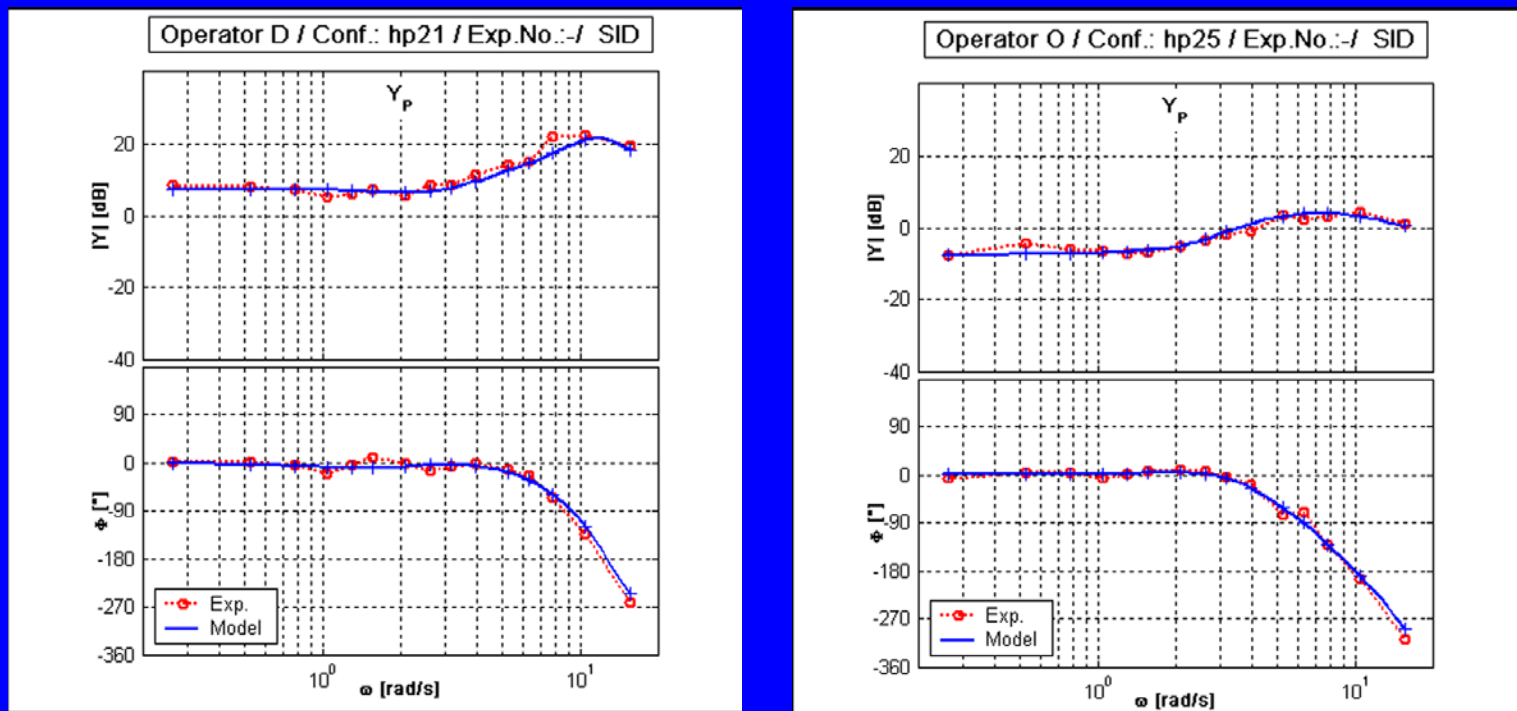
Improved Structural Model Results (Pilot Transfer Function Only Shown)
Fixed-Base Flight Simulator Results

G. Weber

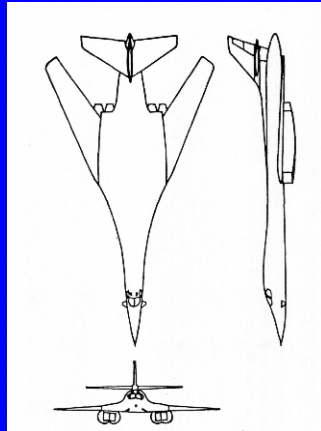
Berlin Technical University (TUB), Berlin, Germany

A.V. Efremov, A.V. Ogloblin

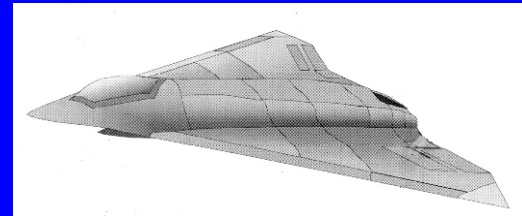
State Technical University – Moscow Aviation Institute (MAI), Moscow,
Russia



Vehicle Examples for Robust Control Design



Flexible B-1



Innovative Control Effector
Vehicle



“Nano” Mesicopter
UAV

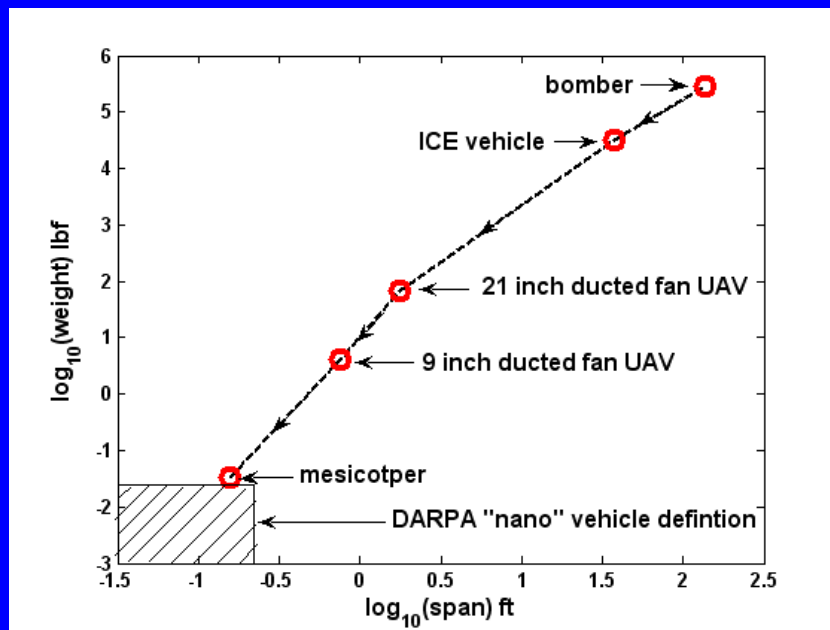


“Micro” 9-Inch
Ducted Fan UAV



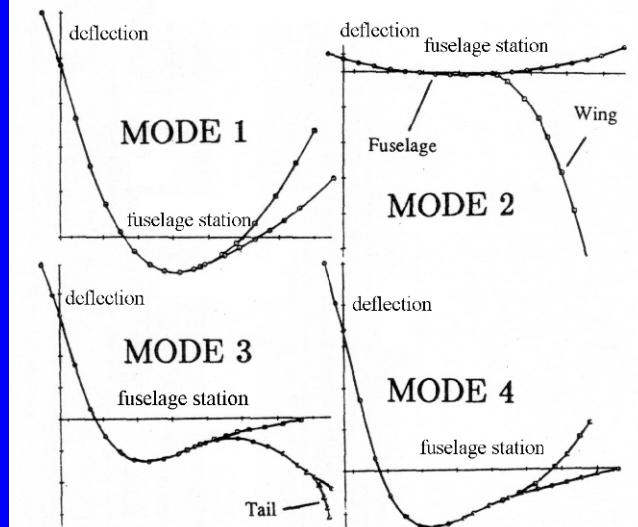
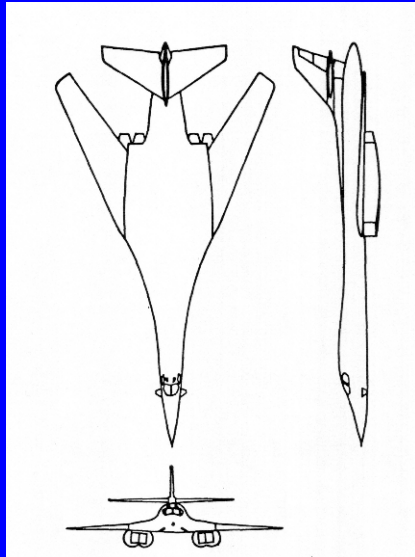
29-Inch Ducted Fan
UAV

Vehicle Examples for Robust Control Design



Size and weight comparison of the example vehicles

Flexible Bomber (longitudinal control)

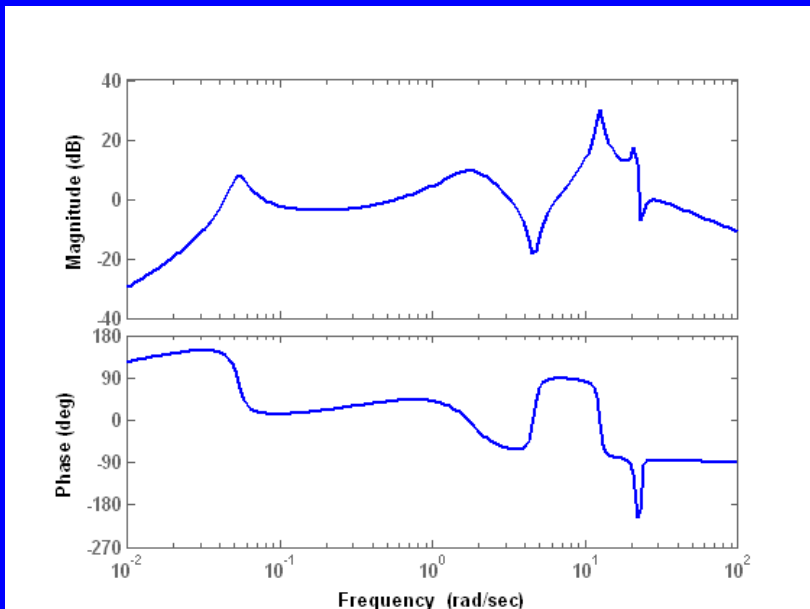


Geometry of the flexible aircraft model

Table 1: Structural Mode Vibration Frequencies of Study Vehicle

Mode 1	Mode 2	Mode 3	Mode 4
12.57	14.07	21.17	22.05
(rad/sec)	(rad/sec)	(rad/sec)	(rad/sec)

Flexible Bomber



Bode plot of $q_{cp}(s)/\delta_{st}(s)$ (1/sec) for the unaugmented aircraft

- (1) The vehicle and actuator models have been obtained. The actuators were amplitude and rate-limited. (only 1st flexible mode included in design)
- (2) A SISO pitch-rate control system is to be designed.
- (3) The sliding manifold is selected as

$$\sigma = e(t) + 22 \int e(t) dt$$

- (4) Sliding behaviour was validated in a computer simulation with

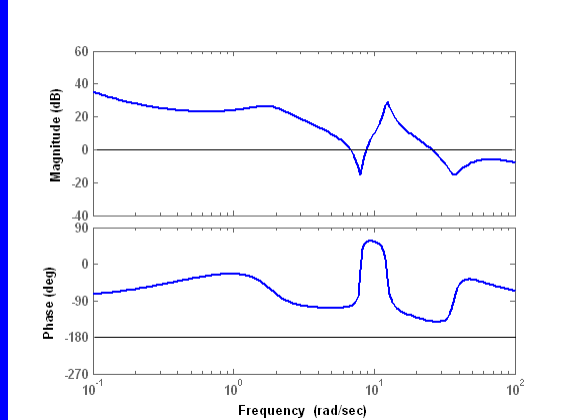
$$u(s) = 3.72\sigma(s)$$

The open-loop crossover frequency was found to be approximately 45 rad/sec

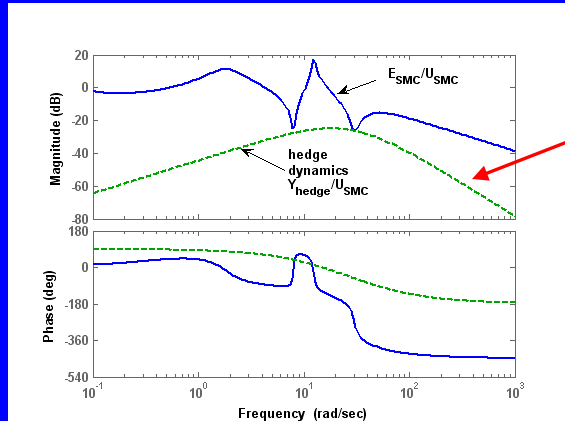
- (5) A boundary layer was created with $\varepsilon = 1.0$
- (6) When actuator dynamics were included, the system was unstable.
- (7) An asymptotic observer was created. The six observer eigenvalues were selected as

$$\lambda_i (i = 1, \dots, 6) = -5, -5.5, -6, -6.5, -7, -7.5 \text{ rad/sec}$$

Flexible Bomber



Bode diagram of $L_{eq}(s)$ for observer eigenvalue selection



Selecting gain on hedge dynamics

(7) Cont'd

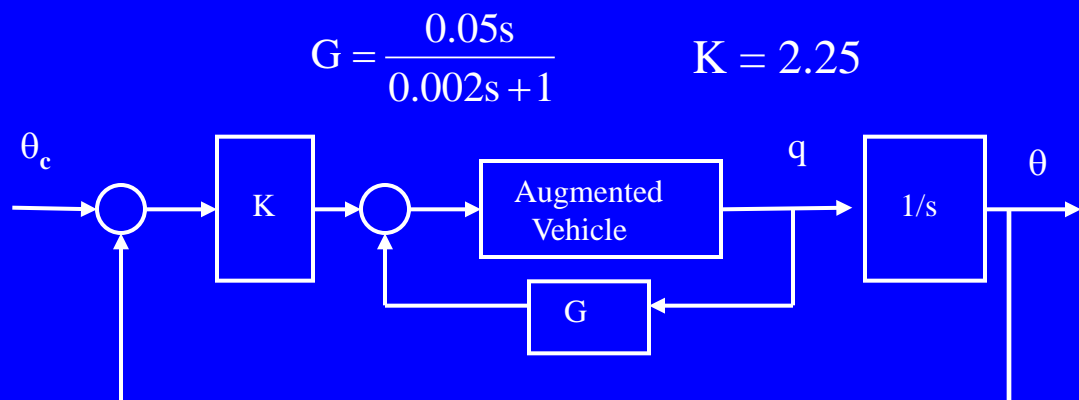
- (a) crossover frequency of 6.82 rad/sec
- (b) infinite gain margin
- (c) 77 deg phase margin

(8) Hedge dynamics were created as

$$G_{\text{hedge}}(s) = \frac{121.4 \cdot s}{s^3 + 90s^2 + 2400s + 20000}$$

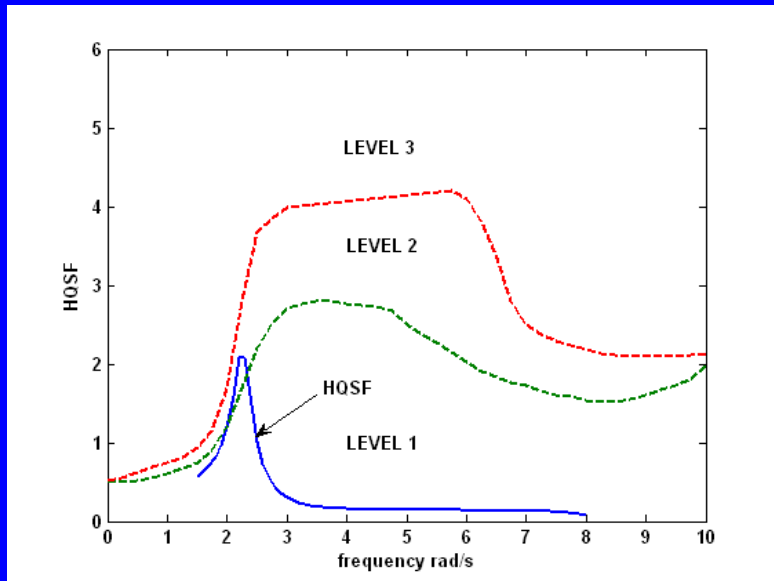
Flexible Bomber

- The observer, itself could not accommodate the significant non-minimum phase dynamics introduced by unmodelled delays
- To add robustness, an additional pitch-acceleration loop was closed around the final pitch-rate command system.
- Finally, an attitude command/attitude hold system response type was created. This is shown below



Flexible Bomber

Handling qualities prediction



HQSF for pilot/vehicle system showing
Level 2 handling qualities prediction

- Failure of the design to achieve predicted Level 1 handling qualities can be attributed to the use of only a single control effector in the pitch-attitude system.
- An improved design approach would incorporate the small control vane near the cockpit as a device dedicated to the suppression of aeroelastic effects sensed at the cockpit.
- Unfortunately, aerodynamic data for the vane was not available

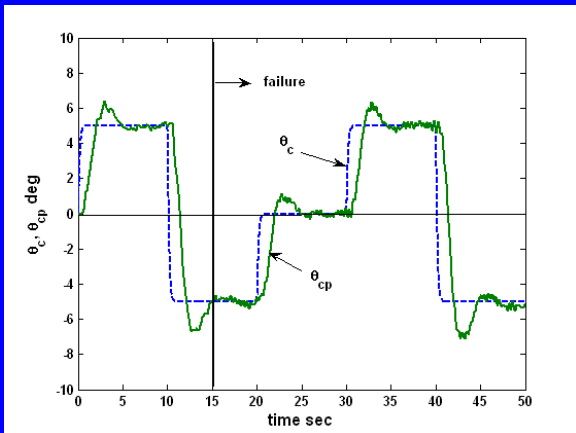
Flexible Bomber

Computer Simulation of Pilot/Vehicle System

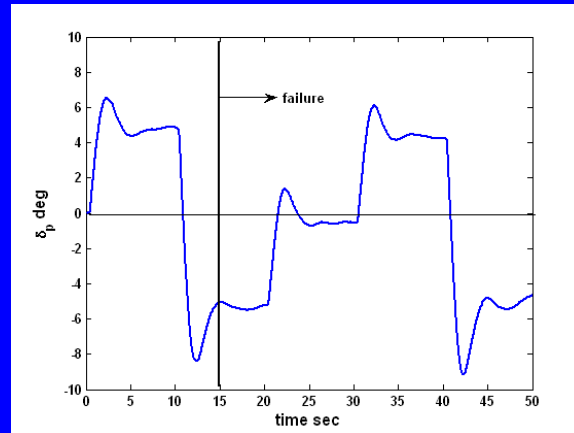
- Complete model utilized with four flexible modes
- Pilot tracking task is following a series of pulsive pitch-attitude commands
- Atmospheric turbulence and sensor noise included
- Unmodelled 0.01 sec time delays introduced before actuators and in sensors
- A “failure” is introduced 15 sec into a 50 sec run by reducing stabilator effectiveness by 25% plus an additional 0.025 sec delay before the actuator

Flexible Bomber

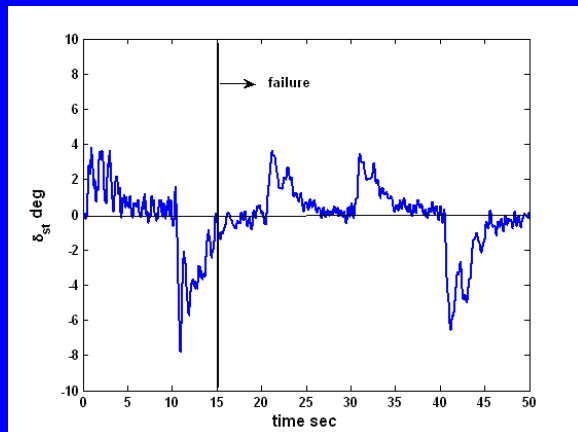
Computer Simulation of Pilot/Vehicle System



pitch-attitude commands and output

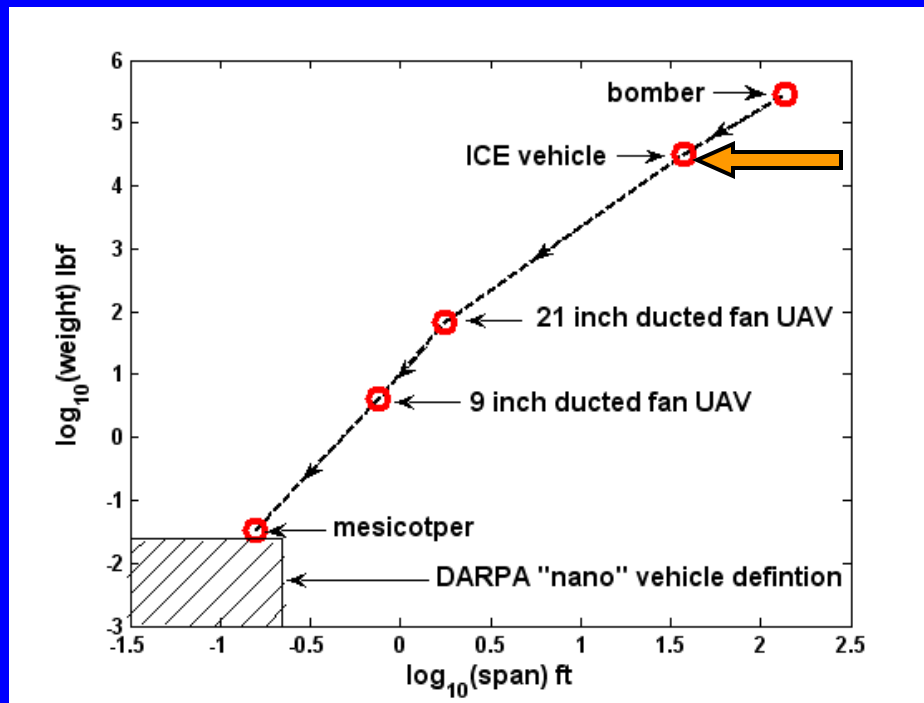


pilot model control inceptor inputs

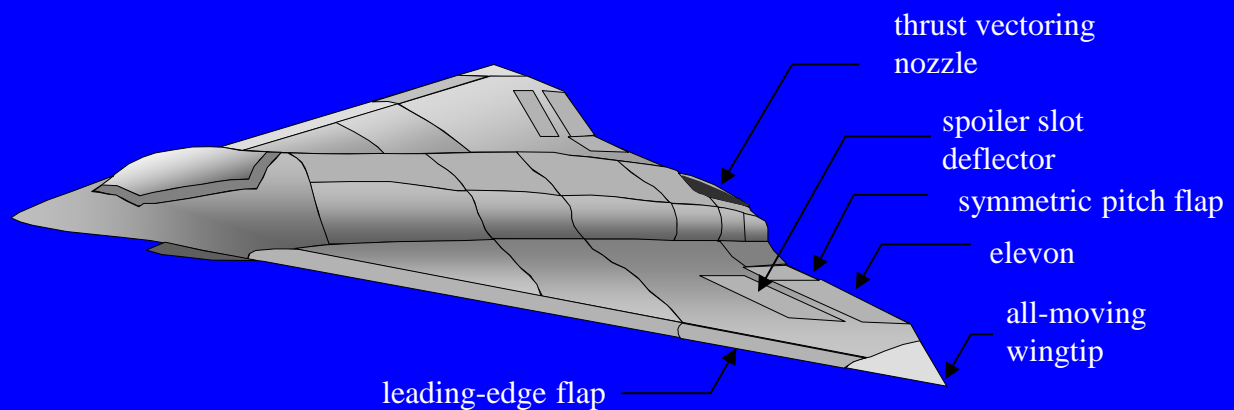


stabilator activity

Innovative Control Effector (ICE) Aircraft



Innovative Control Effector (ICE) Aircraft (longitudinal and lateral control)



The ICE vehicle

Innovative Control Effector (ICE) Aircraft

- (1) The vehicle and actuator models have been obtained. The actuators were amplitude and rate-limited.
- (2) A MIMO pitch-attitude, roll-rate and sideslip control systems are to be designed.
- (3) The sliding manifolds were selected as

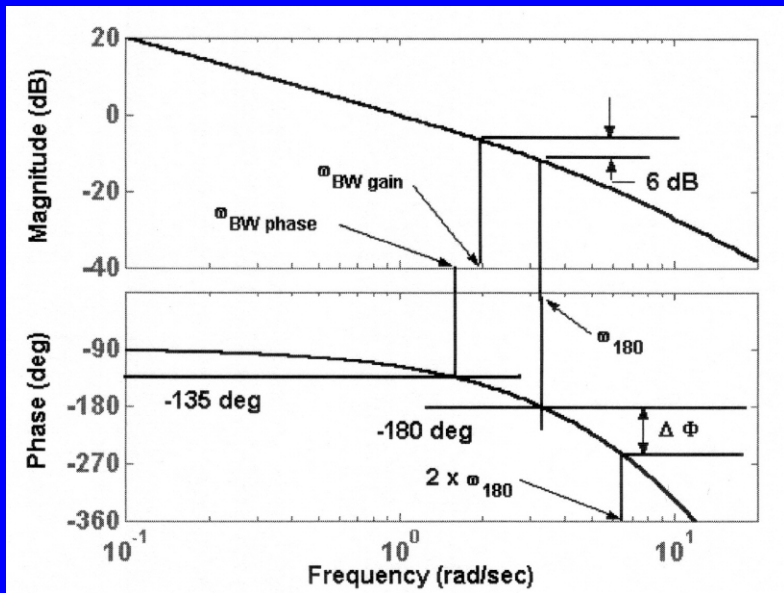
$$\alpha\text{-loop: } \frac{u_\alpha(s)}{\alpha_e} = \frac{5000(s+10)}{s} \quad \beta\text{-loop: } \frac{u_\beta(s)}{\beta_e} = \frac{5000(s+10)}{s}$$

$$p\text{-loop: } \frac{u_p(s)}{p_{s_e}} = \frac{1000(s+10)}{s}$$

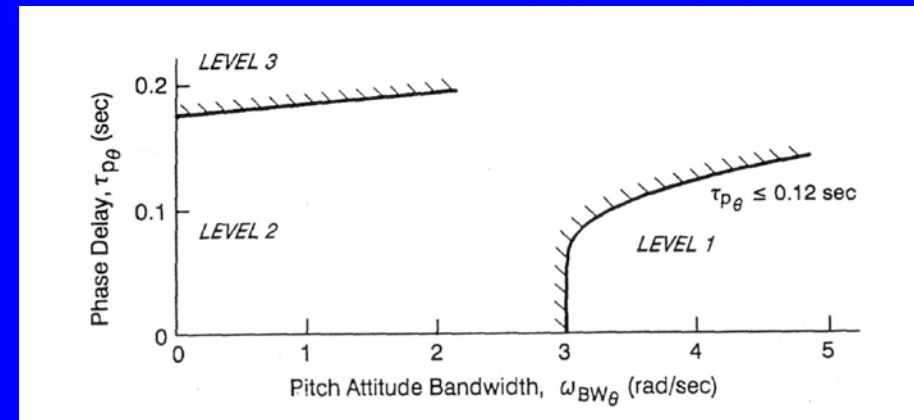
- (4) Sliding behaviour was validated in a computer simulation
- (5) A boundary layer was created with $\varepsilon = 1.0$
- (6) When actuator dynamics were included, the system was unstable.
- (7) An asymptotic observer was created. The observer eigenvalues were selected as
 - α -loop: $\lambda = -1, -1.1, -1.2, \dots, -1.7$ rad/sec
 - p -loop: $\lambda = -10, -10.1, -10.2, \dots, -10.7$ rad/s
 - β -loop: $\lambda = -0.5, -0.51, -0.52, \dots, -0.57$ rad/s
- (8) Hedge dynamics were created as

$$\alpha\text{-loop: } \frac{4s}{s^2 + 4s + 1} \quad \beta\text{-loop: } \frac{4s}{s^2 + 4s + 1} \quad p\text{-loop: } \frac{s}{s^2 + 4s + 1}$$

Innovative Control Effector (ICE) Aircraft



Determining bandwidth and phase delay for pitch and roll handling qualities



Determining handling qualities levels for pitch handling qualities

For the roll axis, the bandwidth determined will be at least 1 rad/sec for Level 1

The phase delay will be no more than 0.14 sec for Level 1 and no more than 0.2 sec for Level 2.

Innovative Control Effector (ICE) Aircraft

Bandwidth/Phase-Delay Results

Mach No. = 0.3, Alt. = 15,000 ft			Mach No. = 0.9, Alt. = 35,000 ft		
	Pitch	Roll		Pitch	Roll
$\omega_{BWphase}$ (rad/sec)	3.69	2.37		3.7	2.3
τ_p (sec)	0.07	0.1		0.07	0.11

All axes predicted as Level 1

Innovative Control Effector (ICE) Aircraft

System damage/failures to be simulated

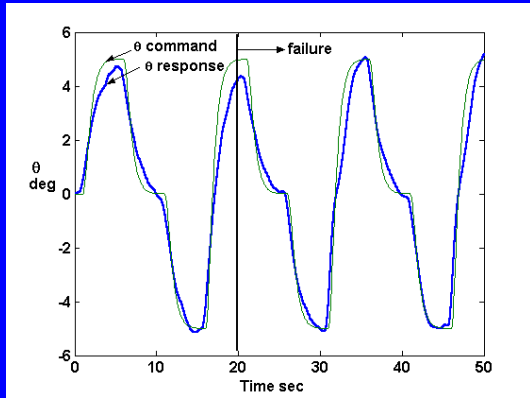
- (1) Left elevon actuator amplitude limits reduced to ± 15 deg; rate limits to ± 15 deg/sec
- (2) Failure 1 plus symmetric pitch flap actuator with hard-over of + 5 deg
- (3) Failures 1-2 plus left spoiler actuator with rate limits reduced to ± 10 deg/sec
- (4) Failures 1-3 plus left leading-edge outboard flap with hard-over of + 5 deg
- (5) Failures 1-4 plus pitch nozzle actuator with rate limits reduced to ± 10 deg/sec
- (6) Failures 1-5 plus elements of the unaugmented plant **A** and **B** matrices each changed by ± 20 percent (excluding kinematic terms)

Innovative Control Effector (ICE) Aircraft

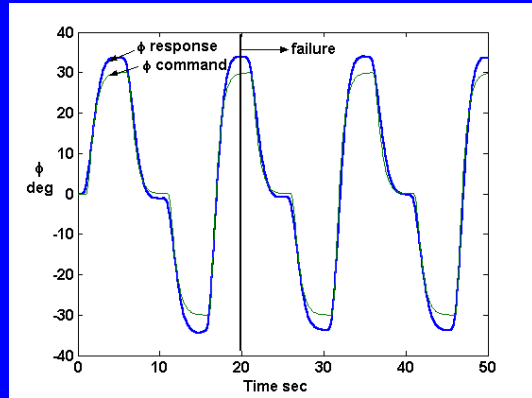
Computer Simulation of Pilot/Vehicle System

- Complete model utilized 13 control effectors
- Pilot tracking task is following a series of pulsive pitch and roll-attitude commands
- Atmospheric turbulence and sensor noise included
- All six failures considered at once
- Two disparate flight conditions considered, but SMC system tuned to only one.
- SMC + observer implemented as discrete controller

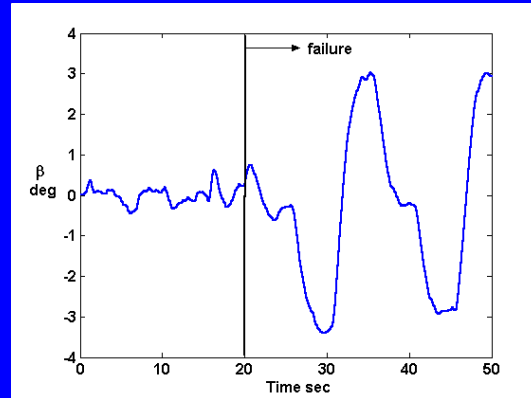
Innovative Control Effector (ICE) Aircraft



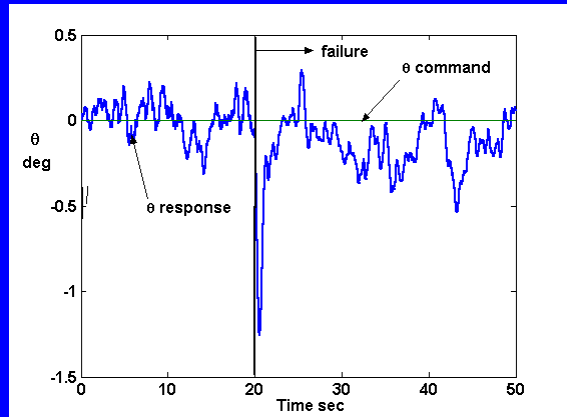
Pitch-attitude tracking, Mach No. = 0.3,
Alt. = 15,000 ft



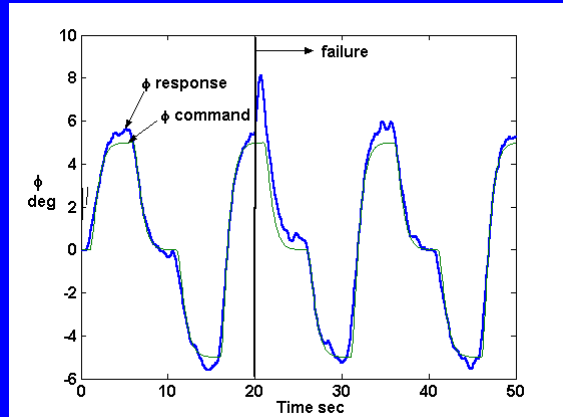
Roll-attitude tracking, Mach No. = 0.3,
Alt. = 15,000 ft



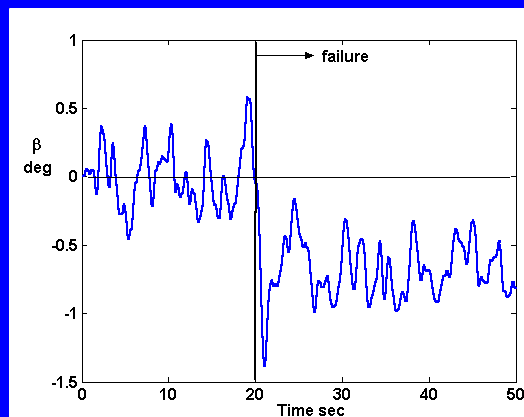
Sideslip regulation, Mach No. = 0.3,
Alt. = 15,000 ft



Pitch-attitude regulation, Mach No. = 0.9,
Alt. = 35,000 ft

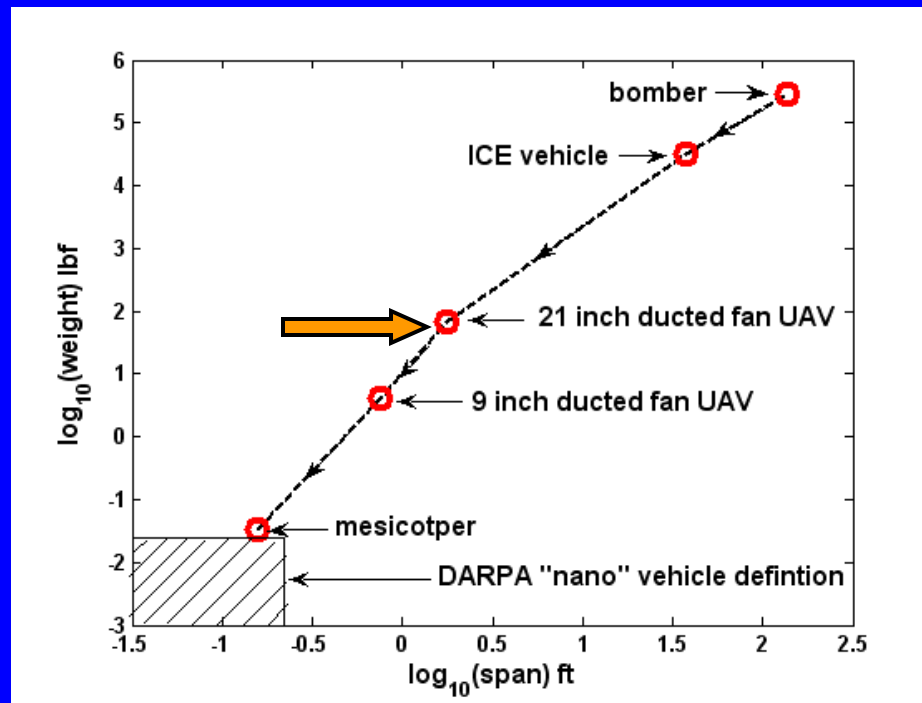


Roll-attitude tracking, Mach No. = 0.9,
Alt = 35,000 ft



Sideslip regulation, Mach No. = 0.9,
Alt. = 35,000 ft

21-Inch Ducted-Fan UAV

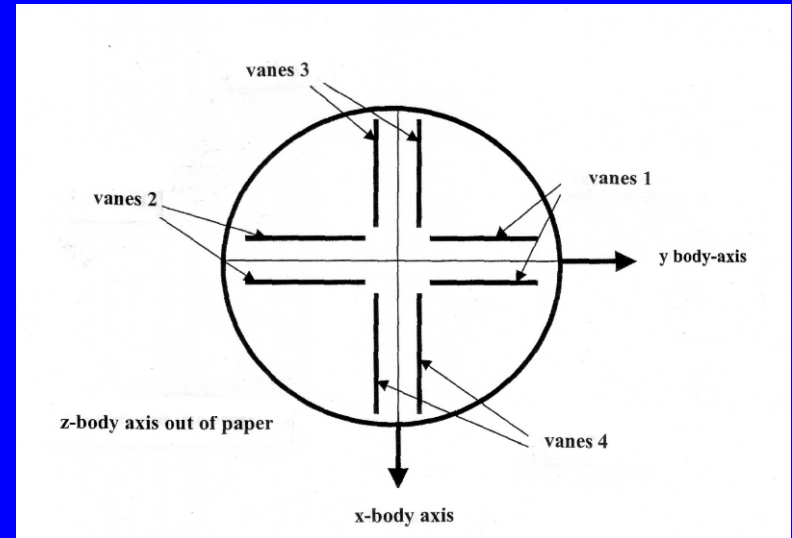


21-Inch Ducted-Fan UAV



A 29-inch UAV

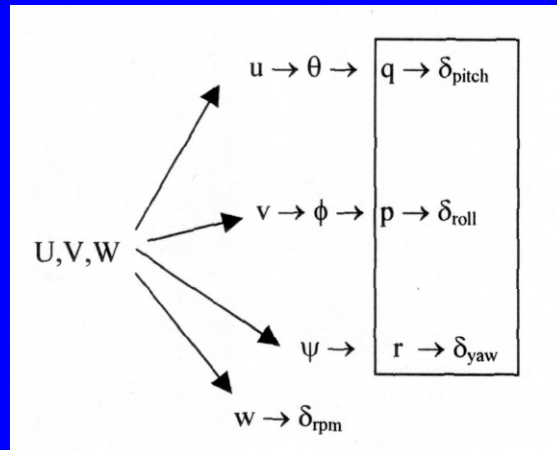
here, z-body axis
is directed out of paper



UAV vane arrangement
Viewed from beneath

21-Inch Ducted-Fan UAV

- Complete nonlinear aero model used in simulation
- Lateral/directional modes subject to control
- Flight velocities from hover to 50 ft/sec
- Outer guidance loops considered (control of velocities in earth-fixed axis system)
- Steady winds, turbulence and sensor noise included in simulation



guidance/control architecture

21-Inch Ducted-Fan UAV

Variation in Linear State Space Matrix Elements Between Hover and 50 ft/sec Flight Conditions

$$\{x\} = [u, v, w, p, q, r, \phi, \theta, \psi]^T; \quad \{u\} = [u_{\text{pitch}}, u_{\text{roll}}, u_{\text{yaw}}, u_{\text{rpm}}]^T$$

A,B matrix elements % change from hover

A(5,1)	-195% (including sign change)
A(4,2)	+32%
A(1,1)	- 46%
A(1,3)	+988% (including sign change)
A(2,2)	-29%
A(3,3)	-94%
B(5,1)	+31%
B(4,2)	+32%
B(6,3)	10%
B(3,1)	-20%

Vehicle dynamically unstable at both flight conditions

21-Inch Ducted-Fan UAV

- (1) The nonlinear vehicle and actuator models have been obtained. The actuators were amplitude and rate-limited.
- (2) A MIMO pitch-rate, roll-rate and yaw-rate control systems are to be designed.
- (3) The sliding manifolds were selected as

$$\text{q-loop: } u(s) = 90 \left[1 + \frac{2}{s} \right] e(s) \quad \text{r-loop: } u(s) = 75 \left[1 + \frac{2}{s} \right] e(s)$$

p-loop

$$u(s) = 150 \left[1 + \frac{2}{s} \right] e(s)$$

SMC controllers designed on basis of linear hover dynamics

- (4) Sliding behaviour was validated in a computer simulation
- (5) A boundary layer was created with $\epsilon = 1.0$
- (6) When actuator dynamics were included, the system was unstable.
- (7) Asymptotic observers were created, one for each loop

21-Inch Ducted-Fan UAV

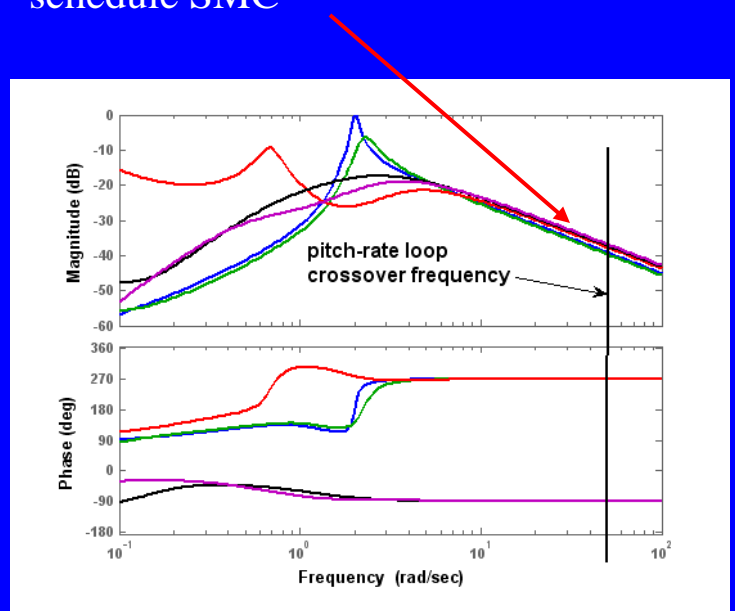
(7) Cont'd The observers each had identical eigenvalues

$$\left. \begin{array}{l} \text{pitch loop:} \\ \text{roll loop:} \\ \text{yaw-rate loop:} \end{array} \right\} \lambda = -5, -5.1, \dots$$

(8) Observer gains scheduled with flight velocity to yield constant eigenvalues across envelope

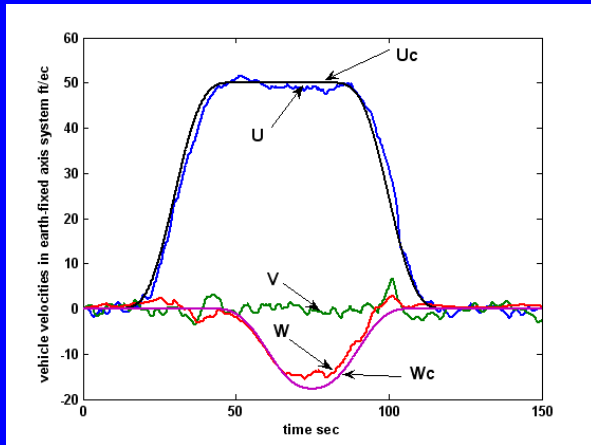
(9) Hedging not employed

nearly identical characteristics
at crossover frequency...no need to
schedule SMC

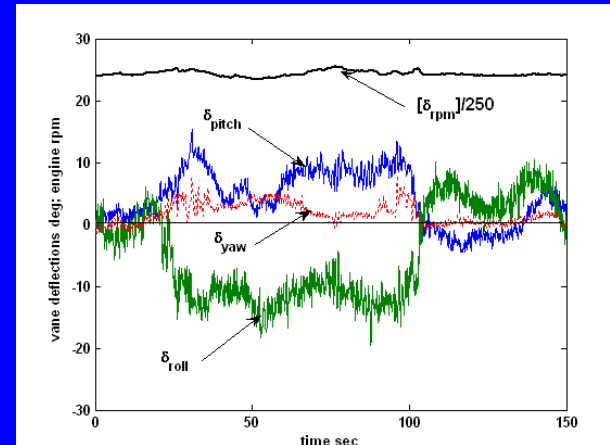


Bode plot of q/u_{pitch} transfer functions
for six trim flight velocities

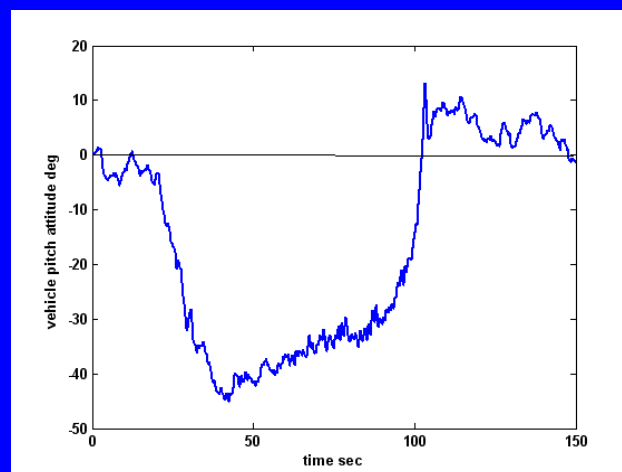
21-Inch Ducted-Fan UAV



vehicle inertial velocity
commands and responses



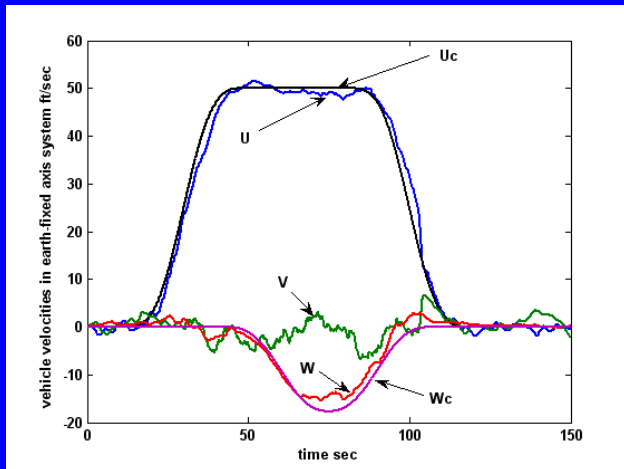
vane deflections and engine RPM



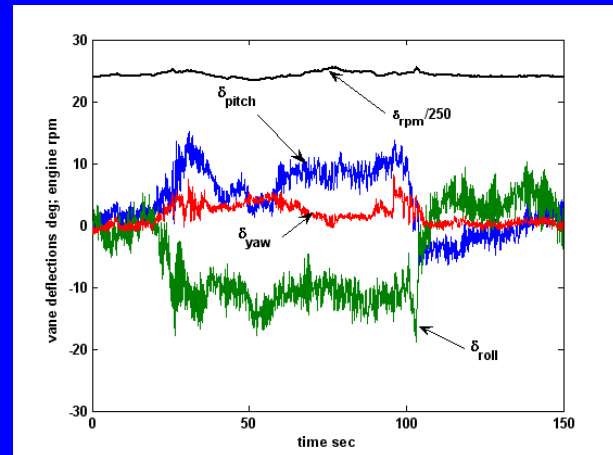
vehicle pitch attitude

21-Inch Ducted-Fan UAV

- Propeller gyroscopic coupling effects added to model
- Only change in SMC design was to increase gains in SMC controller by factor of 2.5
- This change reflected sound frequency domain design principles: to reduce cross-coupling effects, increase crossover frequencies in respective loop transmissions.

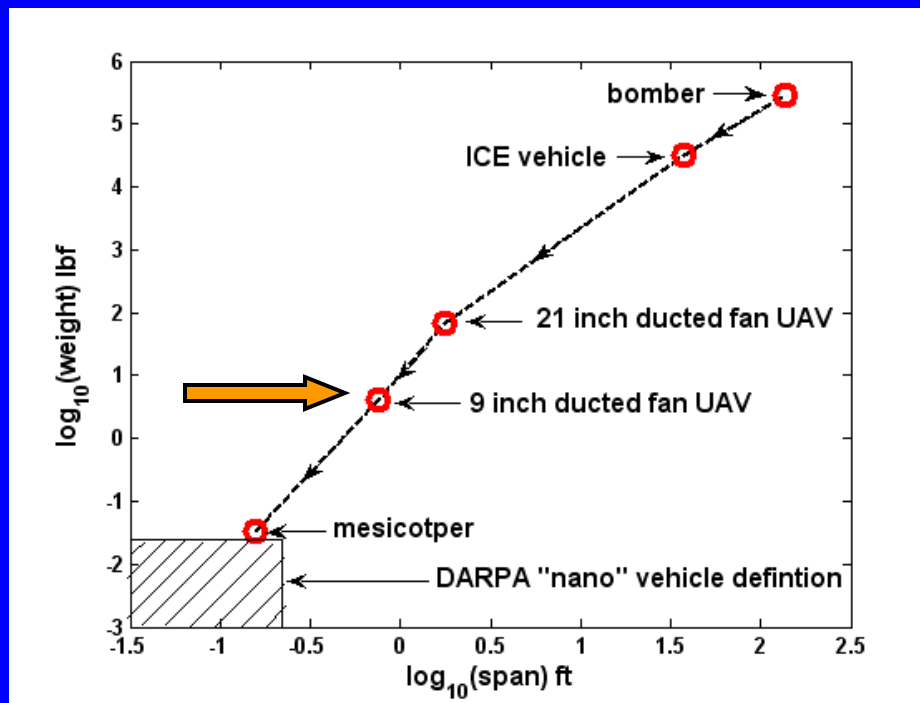


vehicle inertial velocity
commands and responses



vane deflections and engine RPM

9-Inch Ducted-Fan UAV



9-Inch Ducted-Fan UAV

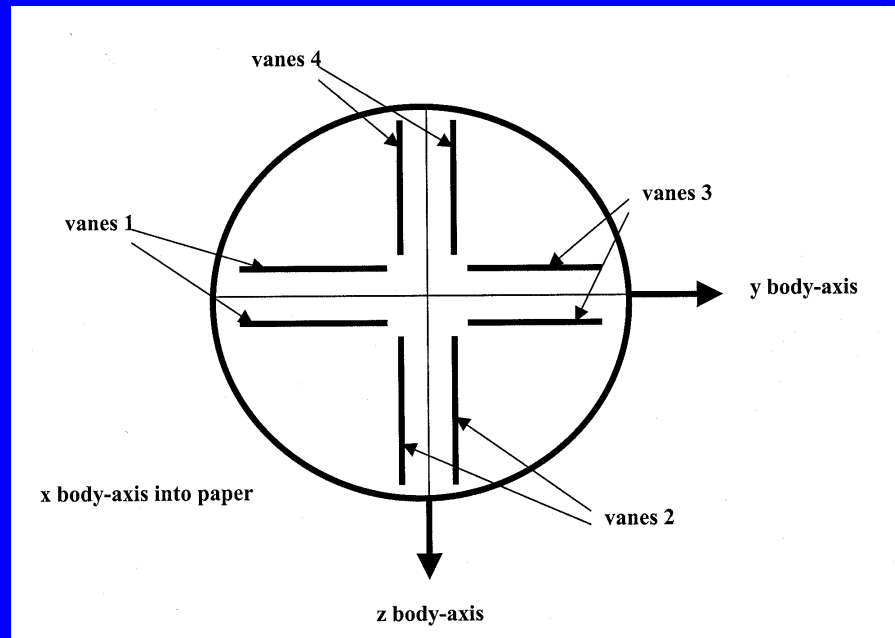
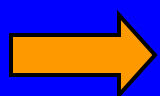


A nine-inch ducted-fan UAV

9-Inch Ducted-Fan UAV

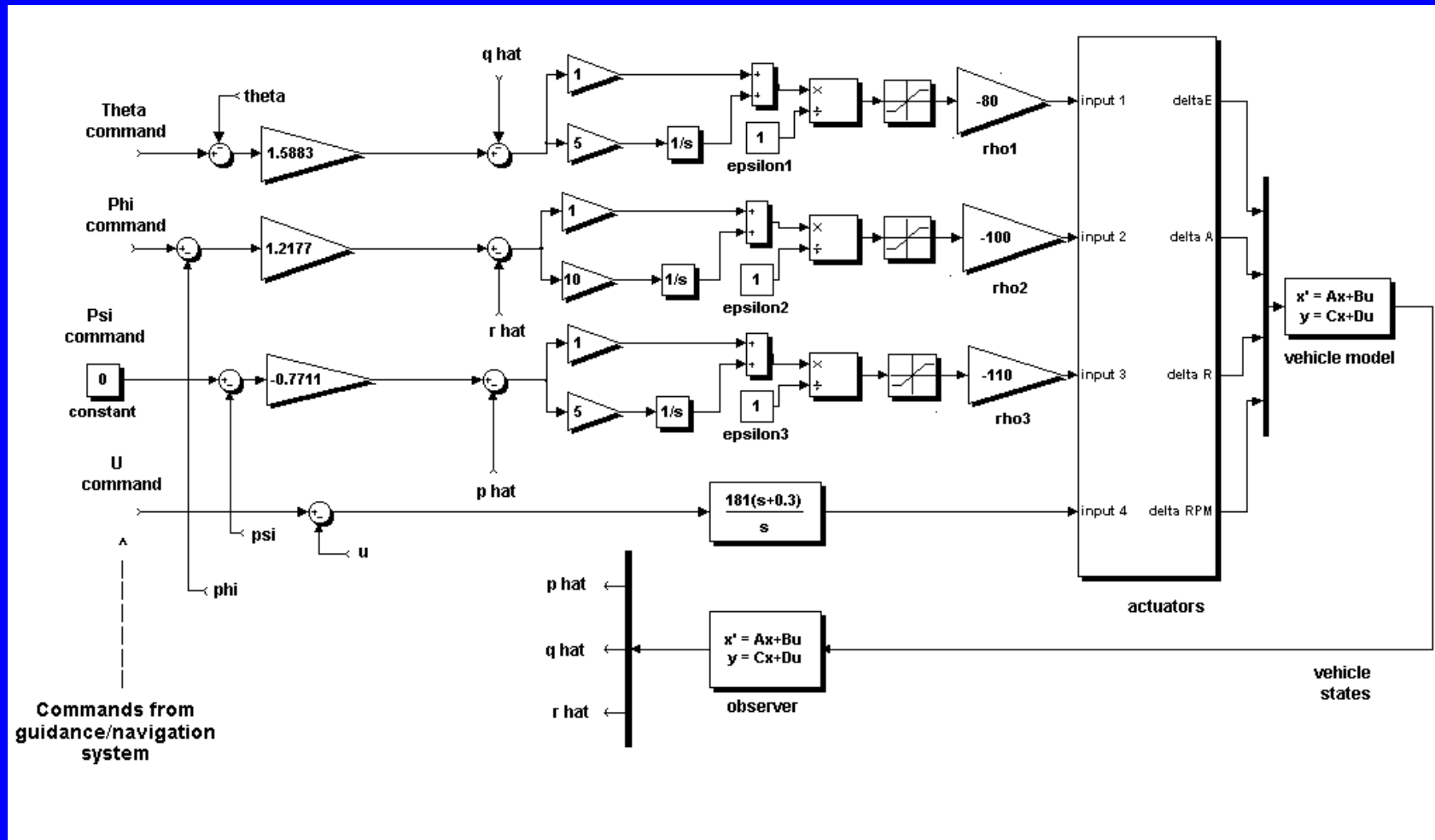
- Linear aero model used in simulation, valid only for low-speed
- Lateral/directional modes subject to control
- Flight velocities from hover to 5-ft/sec
- Outer guidance loops considered (waypoint navigation simulated)
- Turbulence and sensor noise included in simulation

here, x-body axis
is directed into paper



9-Inch Ducted-Fan UAV

Control System Architecture



9-Inch Ducted-Fan UAV

- (1) The linear vehicle and actuator models have been obtained. The actuators were amplitude and rate-limited.
- (2) MIMO SMC pitch-rate, roll-rate and yaw-rate control systems are to be designed.
- (3) The sliding manifolds were selected as

q-loop:

$$u(s) = -80 \left[1 + \frac{5}{s} \right] e(s)$$

r-loop

$$u(s) = -100 \left[1 + \frac{10}{s} \right] e(s)$$

p-loop

$$u(s) = -110 \left[1 + \frac{5}{s} \right] e(s)$$

SMC controllers designed on basis of linear hover dynamics

The open-loop crossover frequencies were 100 rad/sec.

- (4) Sliding behaviour was validated in a computer simulation
- (5) A boundary layer was created with $\epsilon = 1.0$
- (6) When actuator dynamics were included, the system was unstable.
- (7) Asymptotic observers were created, one for each loop

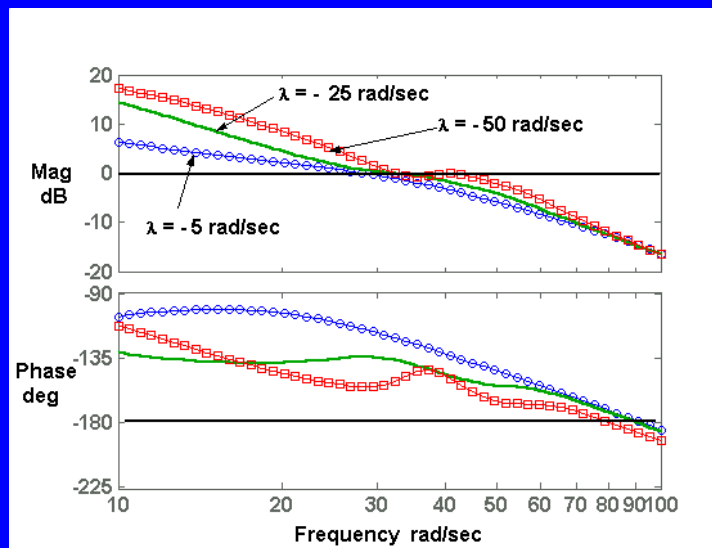
9-Inch Ducted-Fan UAV

(7) Cont'd:

The nine eigenvalues were $\lambda = -25, -25.05, -25.1 \dots -25.4 \text{ rad/sec}$

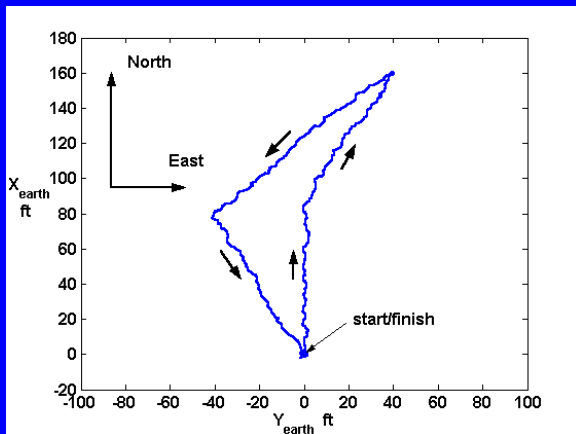
(8) Observer gains NOT scheduled with flight velocity

(9) Hedging not employed

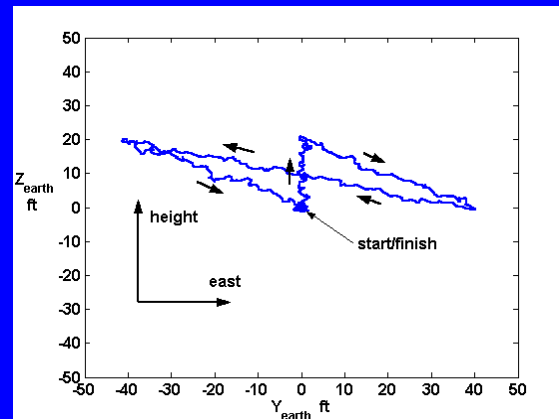


Comparison of equivalent, unity feedback loop transmissions for the pitch-rate loop for different eigenvalue sets

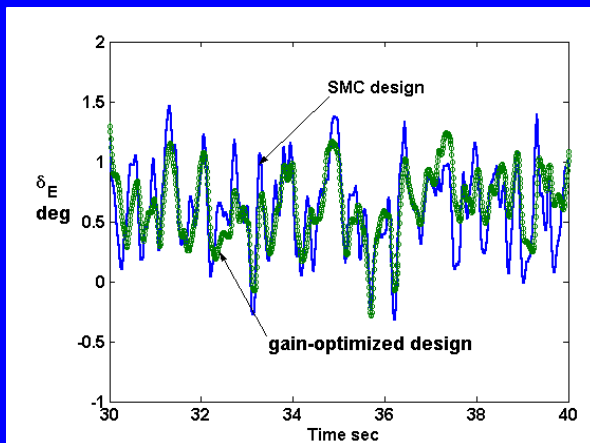
9-Inch Ducted-Fan UAV



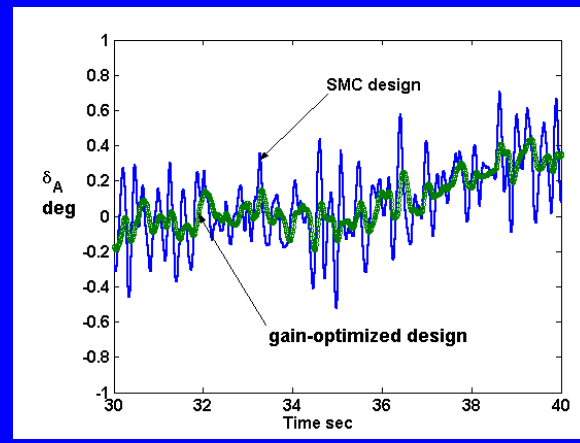
Vehicle trajectory in earth-fixed xy axes



Vehicle trajectory in earth-fixed yz axes

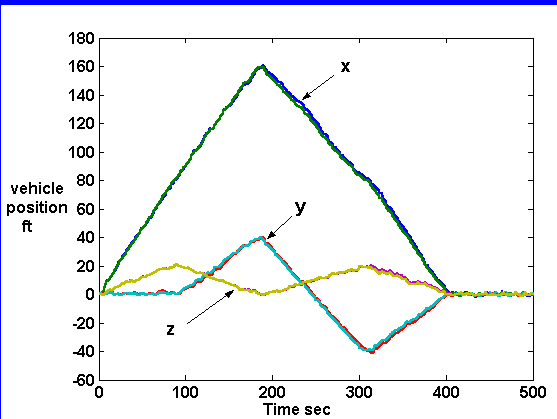


δ_E for gain-optimized and SMC designs

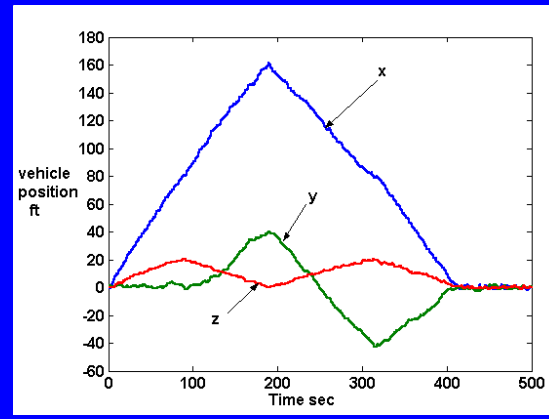


δ_A for gain-optimized and SMC designs

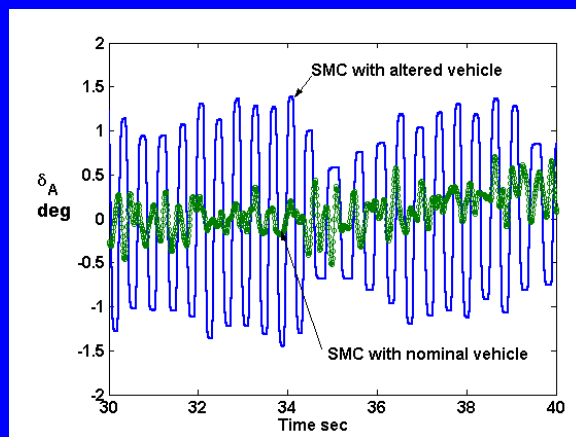
9-Inch Ducted-Fan UAV



Vehicle position for SMC design with nominal vehicle dynamics



Vehicle position for SMC design with altered dynamics and vane actuator deadzone

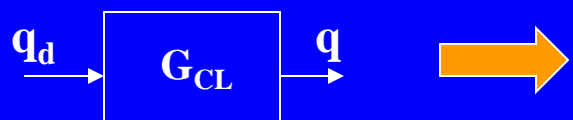


δ_A form SMC design, nominal vehicle and vehicle with altered dynamics and vane actuator deadzone

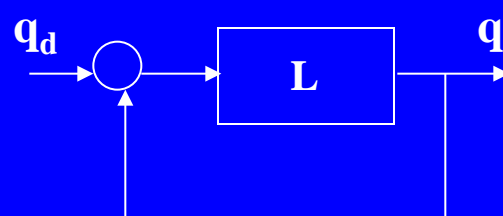
Instantaneous Adaptation?

A common criticism of pseudo-SMC designs is that they are merely fixed-element PID-like compensators - look at “equivalent” compensator:

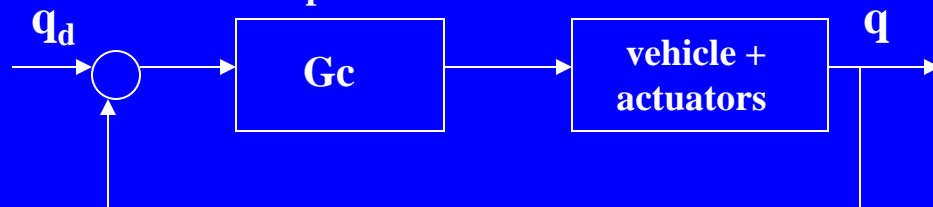
Closed-loop SMC system



$$L = G_{CL}/(1-G_{CL})$$



Equivalent
compensator



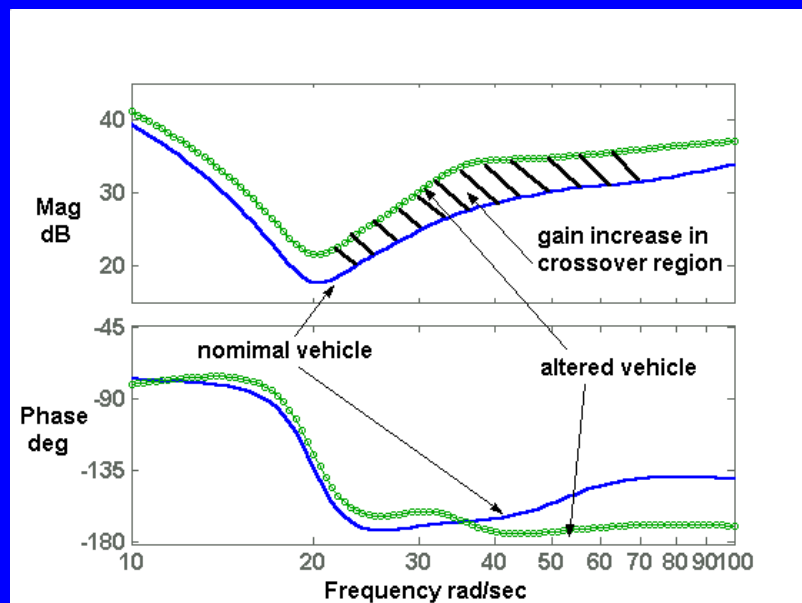
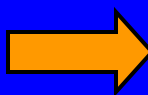
9-Inch Ducted-Fan UAV (instantaneous adaptation?)

$$Gq_c = \frac{L_q}{[q/\delta e_{ac}]^{\prime\prime\prime}}$$

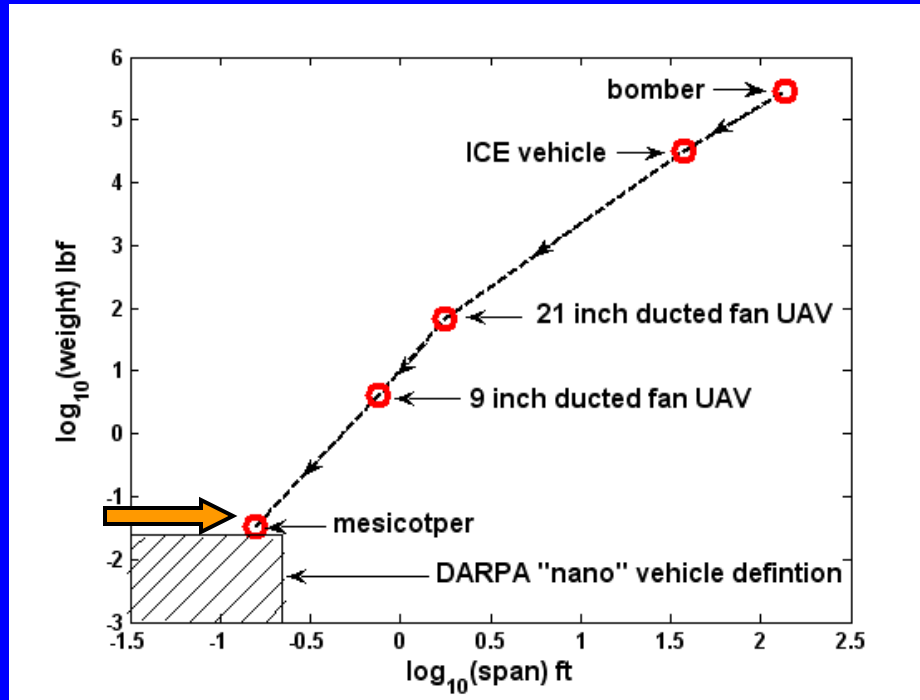
Equivalent unity feedback
loop transmission for q-loop

pitch-rate (q) to elevator actuator
command (δe_{ac}) transfer function
with the remaining three inner-
control loops closed

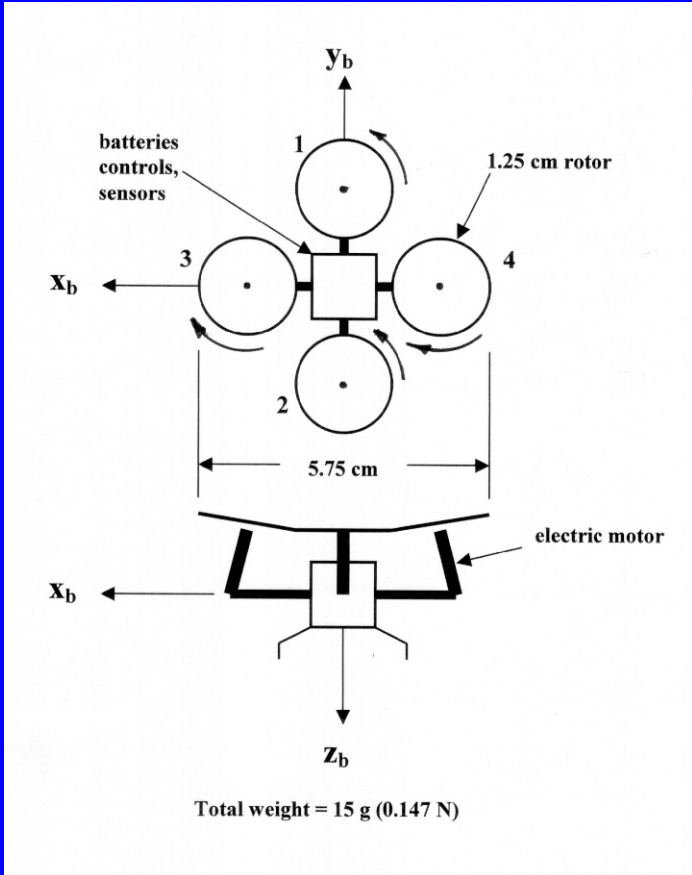
Gq_c before and after elevator actuator
effectiveness reduced by factor of four



Mesicopter (Stanford University)



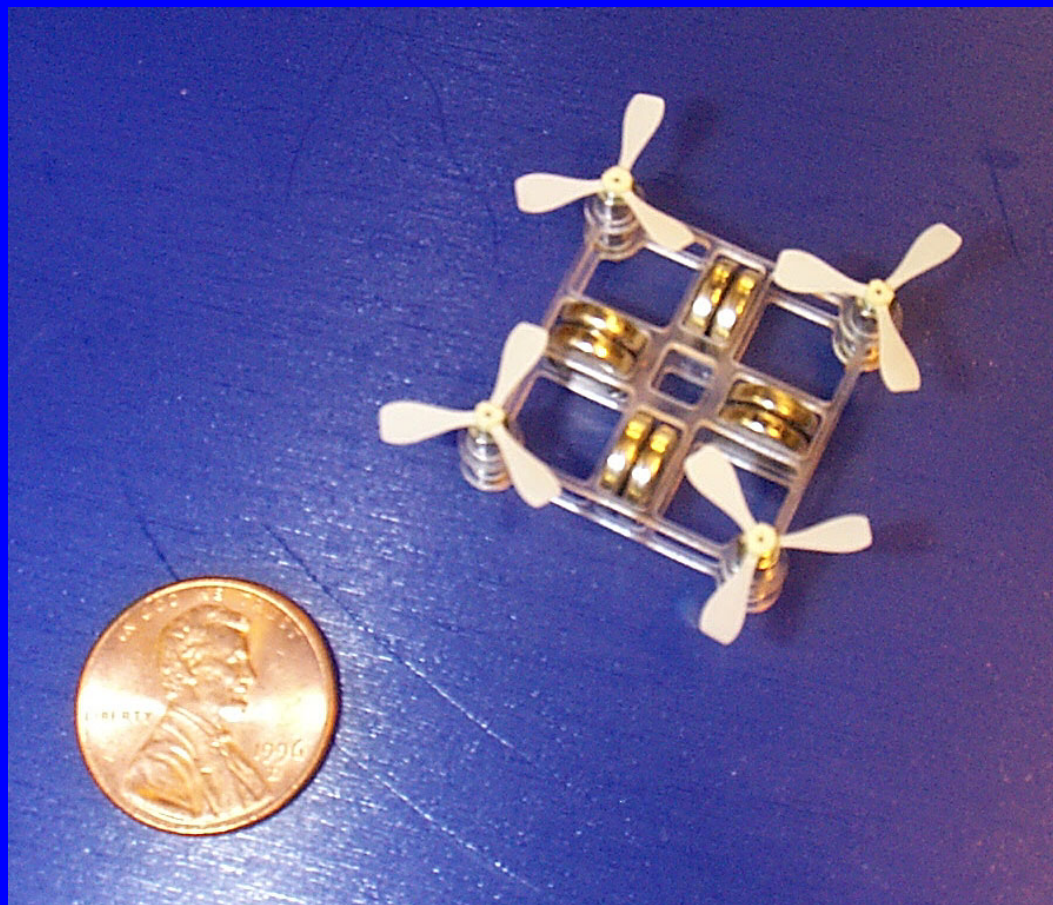
Mesicopter



- Diagonal pairs of rotors, e.g., rotors 1 and 3, spin in opposite directions.
- Pitch inputs are achieved by varying thrust on rotors 1 and 2 and roll inputs are achieved by varying thrust on rotors 3 and 4.
- Vertical thrust is achieved through simultaneous changes in thrust on all rotors.
- Yaw inputs are achieved by increasing (decreasing) thrust on rotors 3 and 4 while decreasing (increasing) thrust on rotors 1 and 2.
- Only longitudinal control studied here.

A notional model of a mesicopter

Mesicopter (Stanford University)



Mesicopter

- (1) The vehicle and motor dynamics have been obtained as described in paper. The electric motors were modelled as second-order “actuators” with both amplitude and rate limiting in terms of angular velocities and accelerations.
- (2) A MIMO control system is to be designed. Here, pitch-rate and z-body axis velocity were the output variables of interest.
- (3) Sliding manifolds were created for each of the control axes. The resulting controllers for each loop are given by:

pitch-rate loop:

$$u(s) = 632 \left[1 + \frac{2}{s} \right] e(s)$$

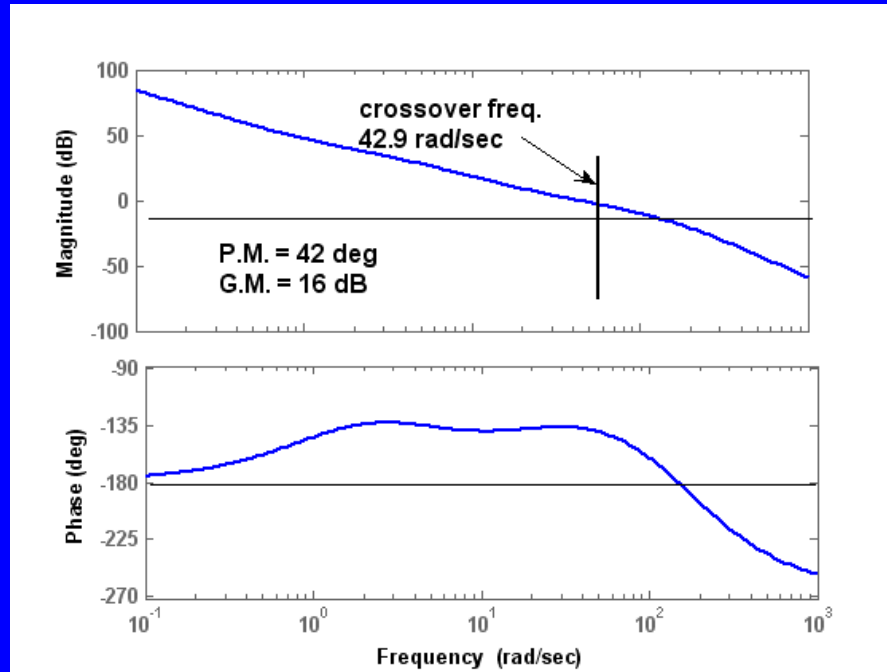
z-body axis velocity loop

$$u(s) = -3.724 \cdot 10^4 \left[1 + \frac{2}{s} \right] e(s)$$

- (4) Sliding behaviour was validated in a computer simulation. The controllers exhibited crossover frequencies of 200 rad/sec.
- (5) Boundary layers of unity thickness were implemented, eliminating the infinite-frequency switching.
- (6) The system was unstable when the motor dynamics (actuators) were included.
- (7) A single asymptotic observer was created to service both of the control loops. In designing the observer, it was assumed that the following measured variables were available - pitch-rate, x-body fixed axis velocity, z-body fixed-axis velocity. The state-space model used to obtain the observer was a minimum realization of the original seven-state vehicle model. The minimum realization resulted in a four-state model. The observer eigenvalues (four) were selected as $\lambda = -20, -20.1, -20.2, -20.3$.

Mesicopter

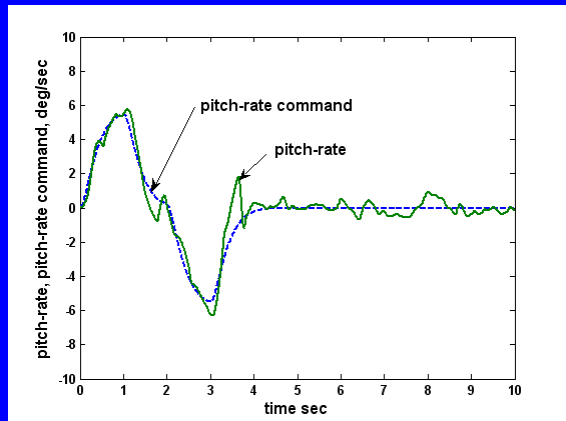
- (8) For simplicity, no reference model hedging was employed in the design.
- (9) Since only flight about hover was considered, no scheduling of the observer was undertaken.



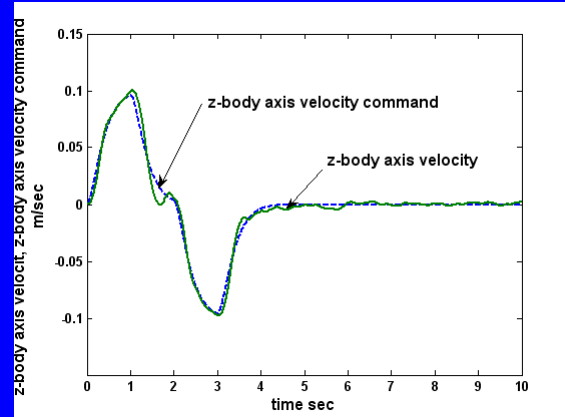
The equivalent, unity feedback loop transmission for the mesicopter z-body axis rate loop

Mesicopter

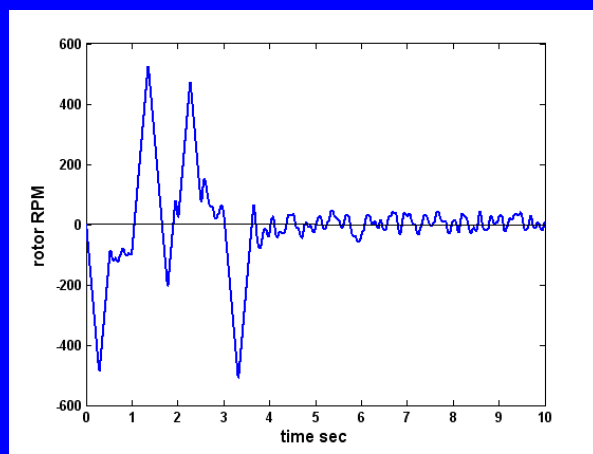
Sensor noise and horizontal turbulence was included with an RMS value of 0.5 m/sec.



Mesicopter pitch-rate performance



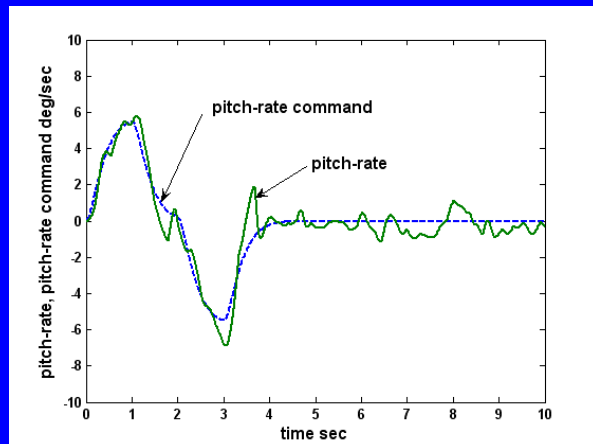
Mesicopter z-body axis velocity performance



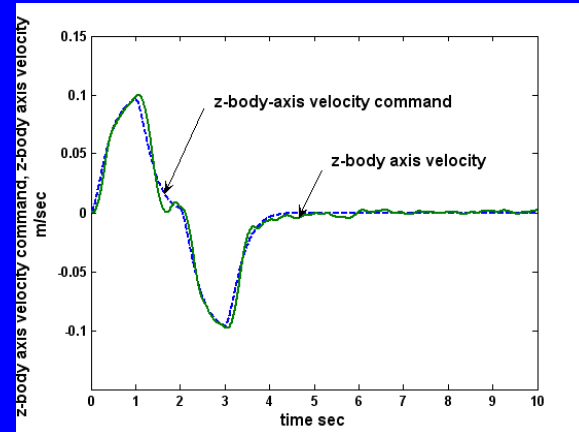
Change in RPM from trim for rotor 1

Mesicopter

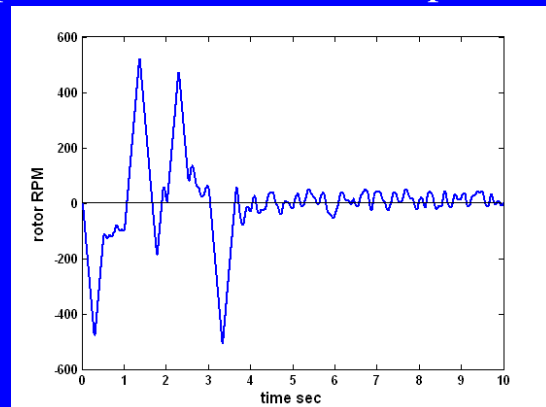
Mesicopter “damage” was modelled by a 25% reduction in the magnitude of the RPM commands to all the motors and inclusion of a 0.015 sec time delay before each motor input



Mesicopter pitch-rate performance



Mesicopter z-body axis velocity performance

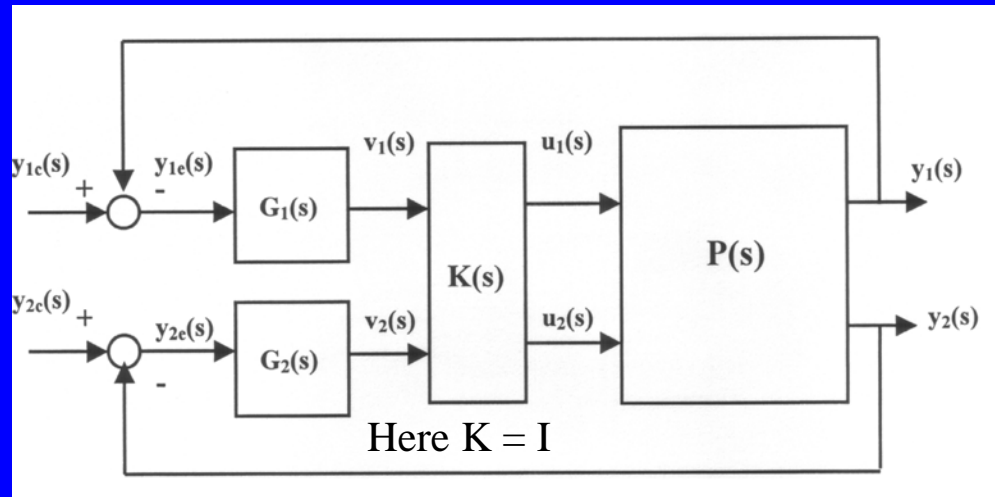


Change in RPM from trim for rotor 1

SMC Design Challenges: RHP Transmission Zeros

Input-Output Pairing and Sequential Loop Closure

Square MIMO system



sequential loop closure with “coupling numerators” assuming constrained responses in loops that are closed

$$\left. \frac{y_i}{u_j}(s) \right|_{y_j \rightarrow u_i} \cong \frac{y_i}{u_j}(s) \cdot \frac{G_i(s) \frac{N_{u_1 u_2}^{y_2 y_1}}{N_{u_j}^{y_i}}}{G_i(s) \frac{y_j}{u_i}(s)} = \frac{y_i}{u_j}(s) \cdot \frac{\frac{N_{u_1 u_2}^{y_2 y_1}}{N_{u_j}^{y_i}}}{\frac{y_j}{u_i}(s)} = -\frac{y_i}{u_j} \cdot \frac{\frac{N_{u_1 u_2}^{y_2 y_1}}{N_{u_j}^{y_i}}}{\frac{y_j}{u_i}}$$

MISO “equivalents” in QFT approach

$$\left. \frac{y_i}{u_j}(s) \right|_{y_j \rightarrow u_i} \cong -\frac{P_{ij}(s) \det P(s)}{P_{ji}(s) [-P_{ij}(s)]} = \frac{\det P(s)}{P_{ji}(s)}$$

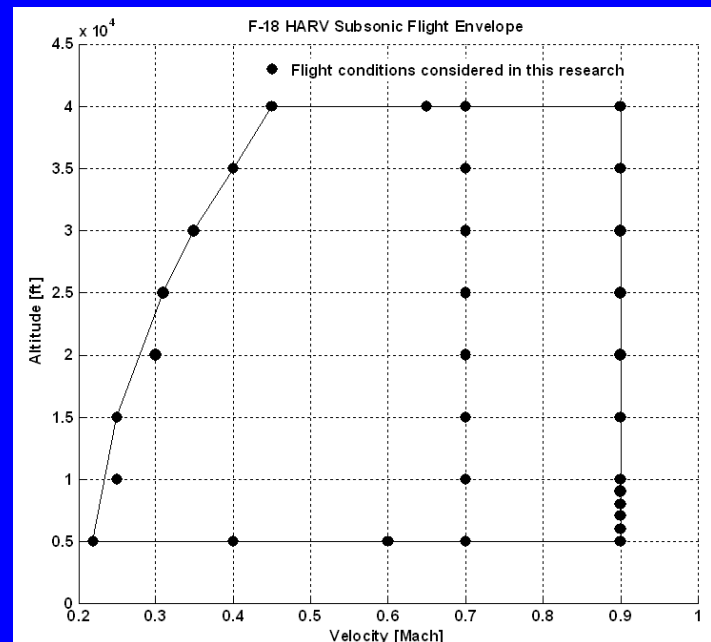
transmission zeros appear here

SMC Design Challenges: RHP Transmission Zeros

Example: Lateral/Directional Control of HARV Model



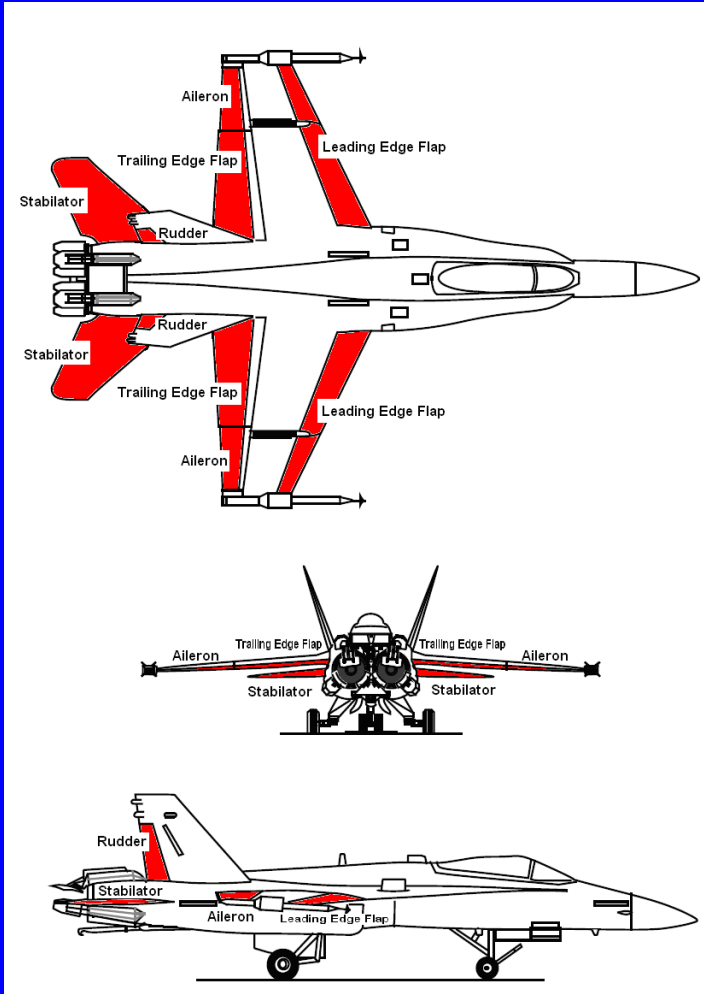
F-18 HARV



Flight Envelope for
Controller Design

SMC Design Challenges: RHP Transmission Zeros

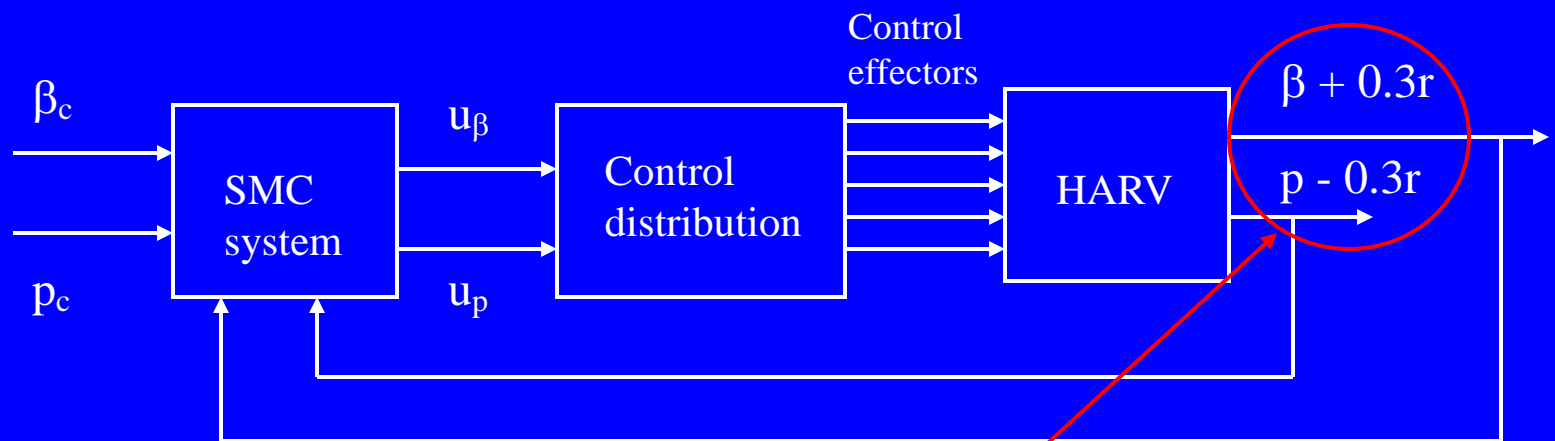
Example: Lateral/Directional Control of HARV Model



$$u = \begin{bmatrix} \delta_{ail} \\ \delta_{ht} \\ \delta_{rud} \\ \delta_{lef} \\ \delta_{tef} \end{bmatrix}$$

Ailerons (deg)
Stabilators (deg)
Rudders (deg)
Leading edge flaps (deg)
Trailing hedge flaps (deg)

SMC Design Challenges: RHP Transmission Zeros



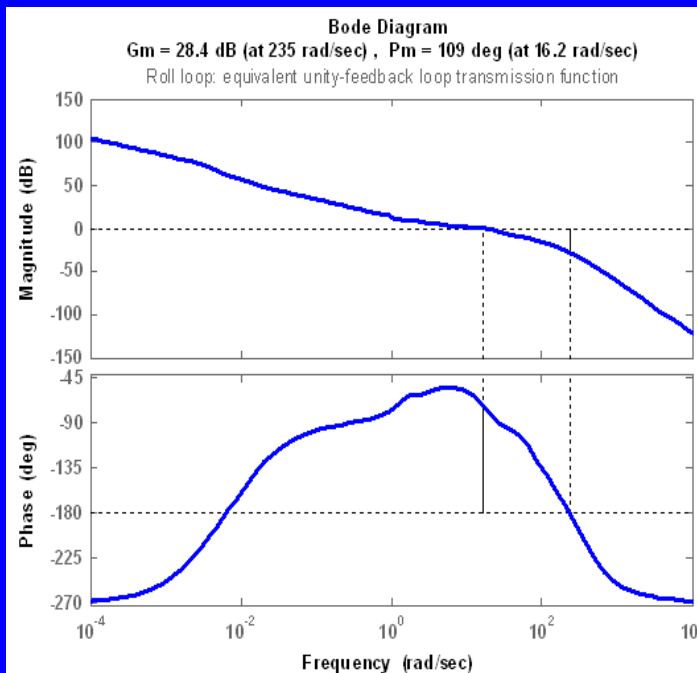
“regulated” variables to
remove RHP transmission
zeros

SMC Design Challenges: Transmission Zeros in Right-Half Plane

Example: Lateral/Directional Control of HARV Model

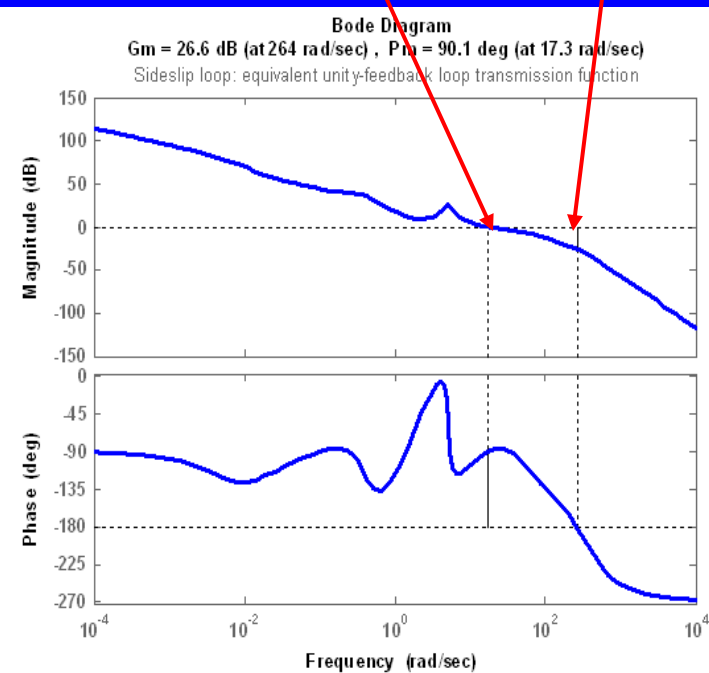
$$u_{\text{roll}}(s) = 75 \left[0.1 + \frac{1}{s} \right] e(s)$$

$$u_{\text{sideslip}}(s) = 60 \left[5 + \frac{1}{s} \right] e(s)$$

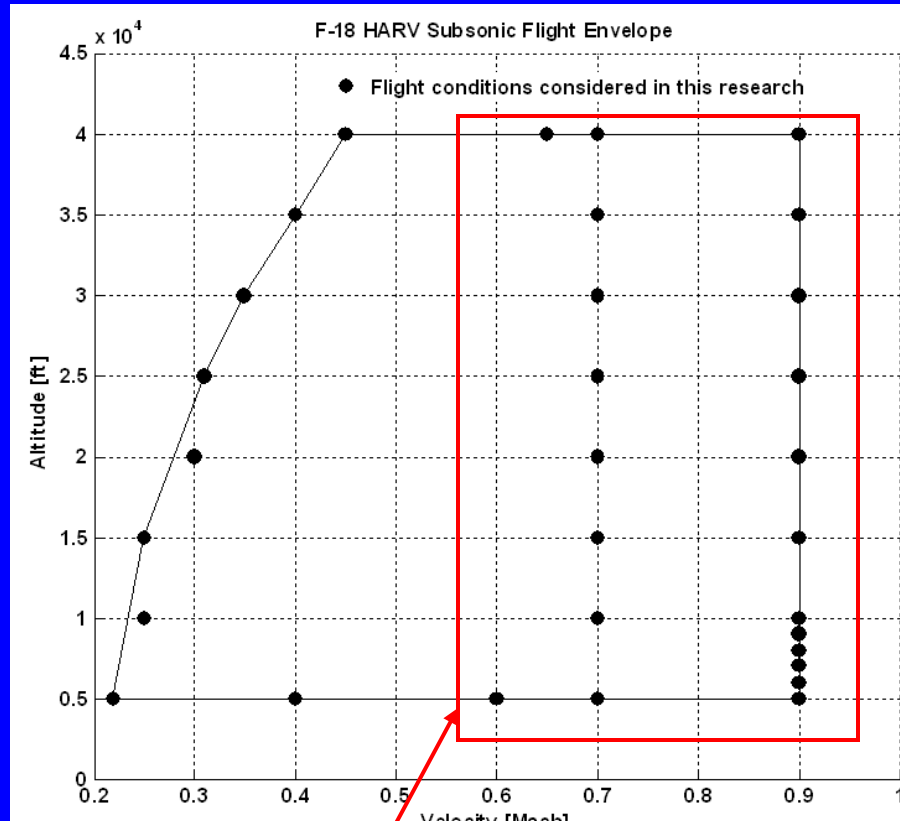


bandwidth after
observer used

bandwidth before
observer used



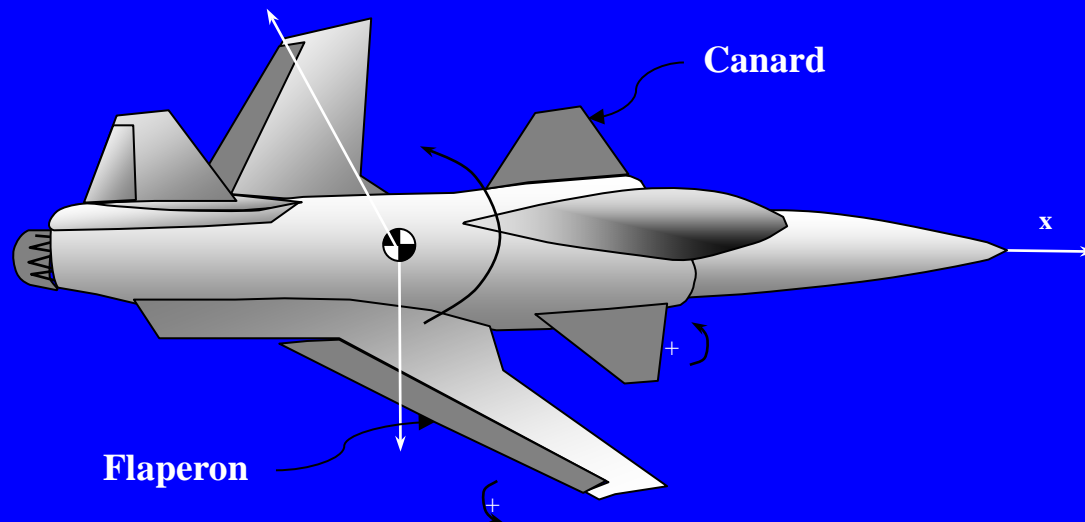
SMC Design Challenges: Transmission Zeros in Right-Half Plane



Configurations stabilized with single SMC design (no scheduling)

Forward Swept Wing Longitudinal Control Example

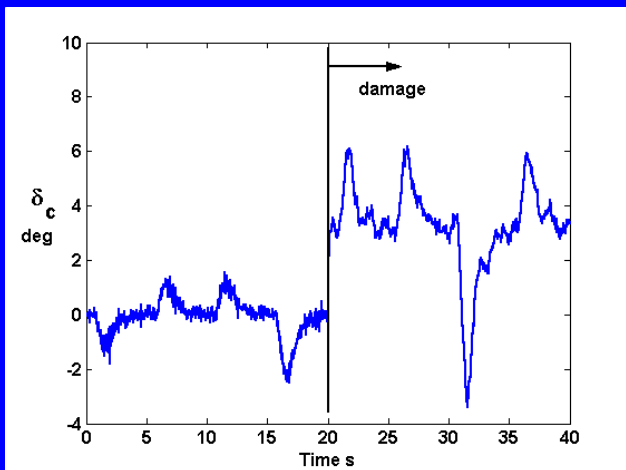
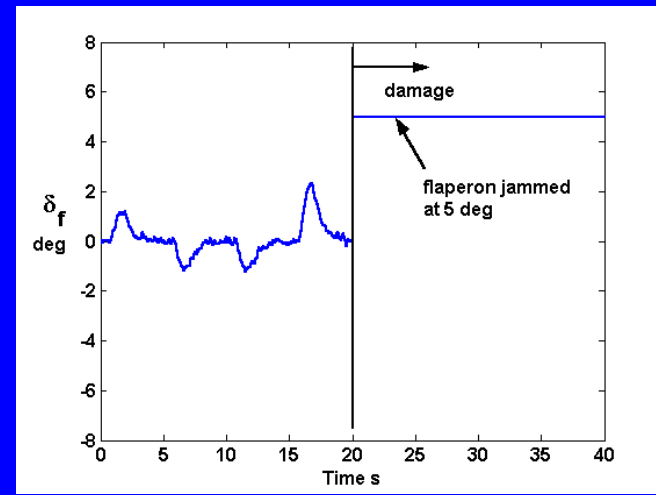
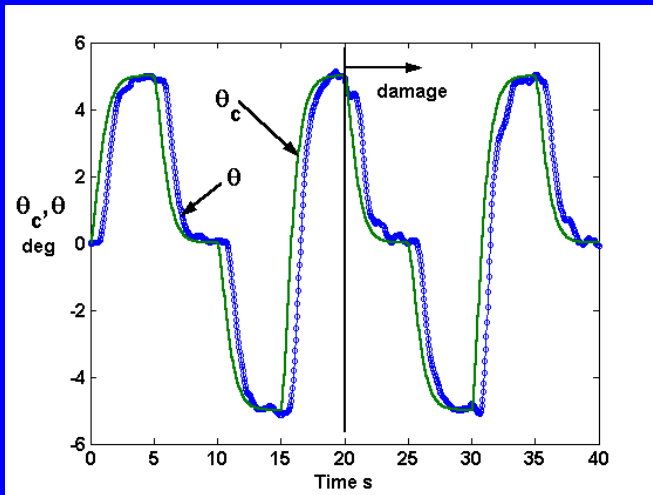
- X-29 - like vehicle from 1982 MS Thesis – Purdue University
- Flexible wing bending mode $\omega_n = 60 \text{ rad/sec}$; $\zeta = 0.165$
- Vehicle possesses aperiodic divergent mode with approx 0.097 sec time to double amplitude



Forward Swept Wing Longitudinal Control Example

- Modeled damage
 - Canard and flaperon actuators operating with 0.025 s added time delay
 - Actuator effectiveness (gain) reduced by 50%
 - Non-kinematic elements in vehicle **A** and **B** matrices perturbed by $\pm 20\%$
 - Flaperon jams at + 5 deg
 - 0.015 sec unmodeled sensor delay
- Flexible mode not modeled in design but included in computer simulation
- Aft-cg vehicle dynamics used in simulation (“center” cg location used in design)
- Pilot model used to follow pulsive pitch-attitude commands

Forward Swept Wing Longitudinal Control Example

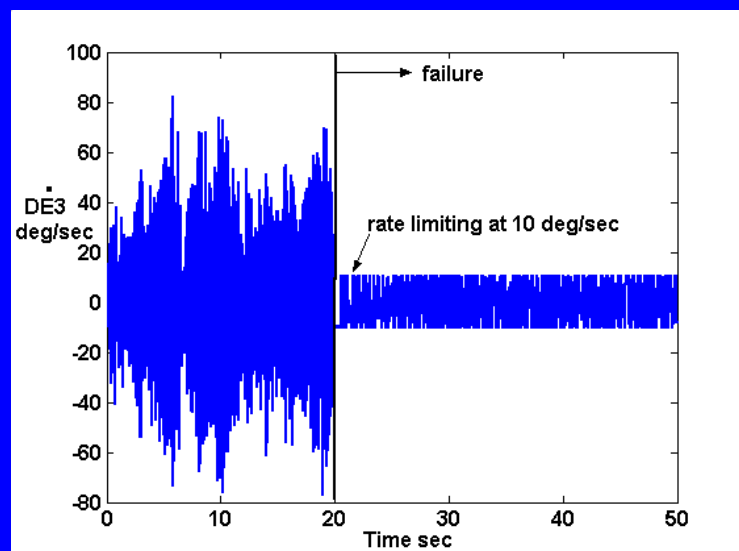


“classical” design went unstable immediately after failure

Stability Proofs?

- Noticeably absent from the proposed design technique are proofs of stability.
- In SMC designs, this question is typically addressed through Lyapunov stability criteria with the goal of guaranteeing global attractiveness of the sliding manifold, i.e. the reaching condition.
- The interpretation of pseudo-sliding mode in the frequency-domain, as done here, merely means that *linear* stability can be ascertained through application of linear techniques such as the Nyquist criterion.
- Guaranteeing stability when the vehicle undergoes significant changes in dynamic characteristics, is quite difficult.
This difficulty is attributable to the fact that the high-bandwidth nature of the SMC approach often results in rate saturation of the actuators, thus eliminating linear stability analyses.

Actuator output rate for ICE vehicle control effectors after cumulative damage. Performance was excellent, however a proof of stability under this condition would be extremely difficult. The author has simply opted for computer simulation to demonstrate stability in these cases



Quantitative Needs

- Design procedure needs a more *quantitative* approach, driven by specific performance requirements and model uncertainty, such as that found in Quantitative Feedback Theory.
- This shortcoming can again be traced to the nonlinear nature of the control activity that often results when the technique is applied to vehicles undergoing significant variations in dynamics due to modelled failures. This obviously remains an area of research.
- The primary design tradeoff that is involved is in the selection of observer eigenvalues and hedge systems.
 - Large eigenvalues bring the design closer to a true SMC system with added robustness to variations in system dynamics. Large eigenvalues also increase the design's sensitivity to the parasitic dynamics of the actuators.
 - Small eigenvalues “hide” the parasitic dynamics of the actuators, but at the cost of some robustness to variations in system dynamics

Summary

- A frequency-domain based approach to the design of sliding-mode flight control systems has been discussed and a number of applications considered.
- The sliding-mode technique served essentially as a means to an end, that being the synthesis of flight control systems that exhibited stability and performance robustness in the presence of significant variations in the vehicle dynamics.
- Since a majority of potential applications of this technique may be to piloted vehicles, some attention has been paid to the description of a control-theoretic model of the human pilot that can be used in computer simulations of the complete pilot/vehicle system.
- The proposed design approach may be particularly advantageous when applied to “nano-scale” UAVs, where on-board computational power may be limited, and where even minor vehicle damage may be enough to cause instability.